CONSTRUCTION CLIMATE CHALLENGE

SCORE - Sustainable Construction Operations for Reduced Emissions

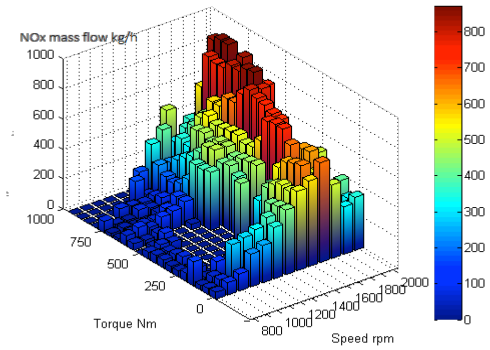

– a prestudy on emission modeling of construction machinery and construction process simulation

Xiaoliang Ma (Project leader)

Traffic Simulation & Control, Department of Transport Science
KTH Royal Institute of Technology

15/12/15

Table of Contents

1. Executive Summary

Heavy construction, as one of the largest industries in civil engineering, is also the major source of pollutants. There is increasing need and interest to achieve sustainable development in the construction area. Quantification of emissions caused by heavy construction is of high importance for improving heavy construction process concerning environmental sustainability. In comparison to the substantial research effort on emissions for road transport, little knowledge has been obtained on how to quantify emissions and model the environmental effects of construction operations, and how to manage and optimize construction processes for reducing emission pollutants. In addition, it is important to investigate the relation between the construction process planning and equipment emissions in real construction operations.

This report summarizes the work carried out within the Construction Climate Challenge pre-study (hosted by Volvo Construction Equipment) project SCORE led by the TSCLab, Department of Transport Science at KTH. Wuhan University of Technology, Beijing University of Technology and Smartways ltd. have been involved as partners in supporting case studies in China. The overall objective of the project is to develop essential models that are dedicated for evaluation of construction induced emissions. The research effort has been mainly devoted to two major topics. The first topic is to measure and model the details emission of construction machinery, a wheel loader in this case. At the test phase, several testing modes are designed to reflect the relationship between emission and various duty-cycles, and an on-board acquisition system is installed to simultaneously log the sensors data. Then, a dynamic NOx emission model is developed to quantify detailed exhaust NOx emissions from construction equipment. Data randomly selected from the database of onboard measurement is applied to calibrate the NOx model. In particular, the engineering characteristic concerning construction operations has been considered to improve the accuracy of the model.

Another essential procedure for quantification and assessment of environmental effects of construction process is the modeling of detailed machine operations and interaction between different construction machinery during construction processes. A discrete-event simulation (DES) tool has therefore been developed in our study to simulate construction cases. It models productivity influenced by factors such as operation efficiency and project schedules. The establishment of DES model also provides a basis for the future integration of the emission model with the DES simulation so that it is technically possible to assess environmental impacts of different construction operations in reality.

2. Introduction

2.1 Background

2.1.1 Construction Emission

Heavy construction is one of the largest industries in civil engineering. The most common construction activities include site preparation, earthmoving (including hauling of material), paving of roadway, the erection of buildings and structures, and even quarries and mining etc. *(1)*. Construction operations can substantially impact local air quality from suspended dust and equipment exhaust. However, because the construction operation is on a regional scale, these pollutants in the zone around non-road construction machinery cannot be reflected from the common published air quality reports made along busy roadways *(2)*. Certain populations that are exposed directly to non-road engine exhaust at greater concentrations than the general population *(3)*. These groups include workers in the construction, timber, mining, and members of the general population that spend a large amount of time near areas where emissions are most densely clustered, such as residents in buildings near large construction sites.

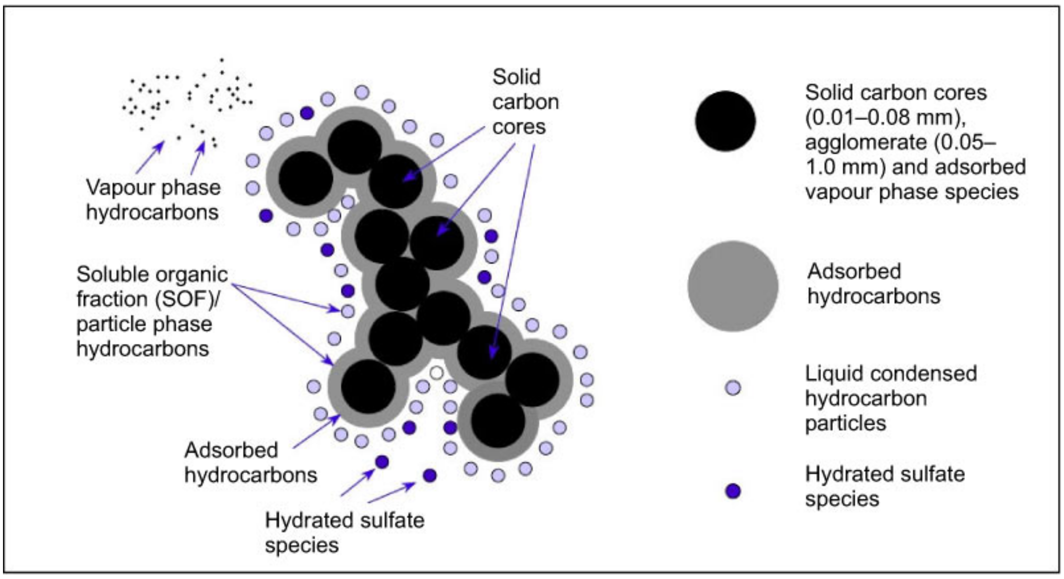

Figure 1 Illustration of engine-out particulate matters (PM)

Considering the characteristic of construction operations, the emissions sources in construction site can be roughly divided as two parts. One part comes from the construction operations itself, such as: earth moving (cut and fill operations, and excavation activities), track-out dirt to nearby traffic, and wind erosion of soil exposed by construction activities *(2)*. Most pollutants in this part belong to suspended dust (also called as particular matters or particulate matters) and vapors from construction material. Such emission usually causes dramatic localized pollution, but it can be directly controlled by construction management policies on site. Such as, conducting watering is effective way to prevent visible dust emissions from exceeding schedule length in any direction *(4)*.

The other source is the emissions from non-road machinery working at the construction site. The term non-road mobile machinery (NRMM) is a term used in the European emission standards to control emissions of engines that are not used primarily on public roadways (5). The non-road standards cover mobile non-road diesel engines of all sizes used in a wide range of construction, agricultural and industrial equipment. Compared to suspended dust, this molecular-level emission is not only easy to disperse, but directly damage human health.

As shown in Figure 1, diesel engines of construction machinery also produce particulate matters (PM), but the engine-out PM is not just the normal suspend dust: engine-out particulate matters (PM) carries stationary carcinogenic polyromantic hydrocarbons (PAHs). As such, diesel particulate matter is almost totally respirable and has a significant health impact on humans. It has been classified by several government agencies as either "human carcinogen" or "probable human carcinogen" *(6)*. Another toxic non-road pollutant is nitrogen oxides (NOx). In areas of construction site, such as in the phase of earth excavation, the amount of nitrogen oxides emitted into the atmosphere as air pollution can be significant. Those small particles can penetrate deeply into sensitive lung tissue and damage it, causing premature death in extreme cases. Inhalation of such particles may cause or worsen respiratory diseases, such as emphysema or bronchitis, or may also aggravate existing heart disease *(7)*. It is also known to increase the risk of heart and respiratory diseases. Non-road engine emissions contain several substances known or suspected as human or animal carcinogens. Except PM and NOx emissions, these other compounds include benzene, 1,3-butadiene, formaldehyde, acetaldehyde, acrolein, dioxin, and polycyclic organic matter (POM). Those non-road diesel engines, contribute significantly to total emissions of these air toxics. All of these compounds were identified as national or regional “risk” drivers worldly. Globally, these compounds pose a significant portion of the total inhalation cancer risk to a significant portion of the population. As discussed later in this section, emission regulations have significantly been reducing these emissions.

2.1.2 Emission Regulations

The fast increase of motor vehicles, not only for road transport but also for non-road construction applications, has raised broad concerns about the need for energy efficiency, global climate change as well as local pollutant emissions and impacts on human health. As a result, antipollution legislation and regulation have become more stringent while the limits on the emission level for motor vehicles are updated continuously. Legislation limiting on-road vehicle emissions has become widespread since 1990, with the permissible emissions levels steadily decreasing with successive legislation *(8)*. For example, the Euro VI regulation of on-road heavy-duty diesel (HDD) engine, similar to the EPA Tier 4 standards, requires almost 80% reduction of the nitrogen oxides (NOx) emission (to 0.4 g/kWh) when comparing to the standards in the previous stage. Table 1 summarizes the pollutant limitations of European Union emission standards on on-road HHD engines, including liquefied petroleum gas (LPG) and spark-ignition natural gas (NG) engines.

The European heavy-duty vehicle and bus engine emission standards apply to all motor vehicles with a ‘technically permissible maximum laden mass’ greater than 3500 kg, equipped with compression-ignition engines or spark-ignition natural gas or liquefied petroleum gas engines *(3)*. The regulations were introduced in tiers from Euro I through to Euro VI, and were revised and consolidated in 2005. The most recent Euro VI standards *(9)*, which become effective in 2013, were published in 2009, and are comparable in stringency to the USA 2010 standards.

Table 1 European Union Euro IV-VI emission standards for on-road heavy-duty engines (g/kWh)

Tier	Year	CO		HC	NMHC	NOx		PM		CH4
		ESC	ETC	ESC	ETC	ESC	ETC	ESC	ETC	ETC
Euro IV	2005	1.5	4	0.46	0,55	3,5	3,5	0,02	0,03	0,03
Euro V	2008	1.5	4	0.46	0,55	2	2	0,02	0,03	0,03
Euro VI	2013	1.6	4	0,13	0,16	0,4	0,46	0,01	0,01	0,01

#PM is not applicable for natural gas (NG) engines at Euro IV stage

#CH4 is for NG engines only (Euro IV-V: NG only; Euro VI: NG and LPG)

Notably, the engines installed in non-road mobile machinery also contribute greatly to air pollution by emitting carbon oxide (CO), hydrocarbons (HC), nitrogen oxides (NOx) and particulate matters (PM). Following the steps of on-road standards, emissions from these engines are regulated before they are placed on the market by six directives: the Directive 97/68/EC, and the amendments: Directive 2002/88/EC, Directive 2004/26/EC, Directive 2006/105/EC, Directive 2011/88/EU, and the recent amendment Directive 2012/46/EU (EC 2014) *(10-15)*. Compare current European non-road and on-road standards, the emission limits maintain almost the same levels in most European countries *(11).*

Table 2 European Union emission standards for non-road engines and equipment (g/kWh)

Year	Rated Power (kW)	CO	HC	NOx+HC	PM
Stage IIIA					
2006	130≤P≤560	3,5	---	4	0,2
2007	75≤P≤130	5	---	4	0,3
2008	37≤P≤75	5	---	4,7	0,4
2007	19≤P≤37	5,5	---	5,7	0,6
Stage IIIB					
2011	130≤P≤560	3,5	0,19	2	0,025
2012	75≤P≤130	5	0,19	3,3	0,025
2012	56≤P≤75	5	0,19	3,3	0,025
2013	37≤P≤56	5	---	4,7	0,025
Stage IV					
2014	130≤P≤560	3,5	0,19	0,4	0,025
2014	56≤P≤130	5	0,19	0,4	0,025
Stage V					
2019	56≤P≤560	3,5	0,19	0,4	0,015

The European standards for non-road engine emissions are proposed in gradually more stringent tiers known as Stages I–V (see Table 2). Emission standards can also be adopted for small, gasoline non-road engines. Stage I began in 1999 and then Stage II was implemented from 2001 to 2004, depending on the size and the power output of the engine. Further technical details on testing methods were adopted for Stage IIIB and Stage IV, and amendments were made to the rules applied to wider scope of non-road machinery. Stage III standards were divided into IIIA and IIIB and were phased in from 2006 to 2013. The Stage V standards would target particle number limits (PN) rather than particulate mass (PM) limits and normalize engines in the 56–560 kW range, which provide new research direction to non-road diesel emissions.

kW	Hp	2001	2002	2003	2004	2005	2006	2007	2008	2009	2010	2011	2012	2013	2014	2015
19-36	25-49	8.0 1.5 0.8						7.5 0.8								
37-56	50-74				7.0 1.3 0.4				4.7 0.4					4.7 0.025		
57-74	75-98				7.0 1.3 0.4				4.7 0.4				3.3 0.19 0.025			0.40 0.19 0.025
75-129	100-174			6.0 1.0 0.3				4.0 0.3					3.3 0.19 0.025			0.40 0.19 0.025

EU - LEGEND	Stage I	Stage II	Stage III A	Stage III B	Stage IV

(a)

kW	Hp	2001	2002	2003	2004	2005	2006	2007	2008	2009	2010	2011	2012	2013	2014	2015
19-36	25-49				7.5 0.6				7.5 0.3					4.7 0.03		
37-56	50-74				7.5 0.4				4.7 0.3					4.7 0.03		
									4.7 0.3				4.7 0.03			
57-74	75-98				7.5 0.4				4.7 0.4				3.4 0.19 0.02			0.4 0.19 0.02
75-129	100-174			6.6 0.3				4.0 0.3					3.4 0.19 0.02			0.4 0.19 0.02

EPA - LEGEND	Tier 1	Tier 2	Tier 3	Tier 4 interim	Tier 4 Final

(b)

EXAMPLES
NOx 2.0 – 2.0, the maximum amount of nitrogen oxide (NOx) allowed in grams / kWh
NMHC 0.19 -0.19, the maximum amount of non-methane hydrocarbons (NMHC) allowed in grams / kWh
PM 0.025 – 0.025, the maximum amount of particulate matter (PM) allowed in grams / kWh

NMHC + NOx 7.5 – 7.5, the maximum amount of NMHC + NOx allowed in grams / kWh
PM 0.8 -0.8, the maximum amount of PM allowed in grams / kWh

Figure 2 Non-road emissions regulation between the EU (a) and EPA Tier (b)

Current US and EU emission standards are equivalent for the 19 kW to 560 kW power rating range. As shown in Figure 2, European Stage I and II limits were harmonized in part with regulations in the USA, and then Stage III and IV limits were harmonized with the USA Tier 3 and Tier 4 standards *(12)*. Regulatory authorities have been under pressure from engine and equipment manufacturers to harmonize worldwide emission standards, in order to streamline engine development and emission type approval/certification for different markets. On May 11, 2004, EPA signed the final rule introducing Tier 4 emission standards, which are phased-in over the period of 2008-2015. Roughly, under the emissions limitation, the Tier 4 is divided into two periods, the Tier 4 interim and The Tier 4 finals. As listed in Table 3, EPA allows the manufactures stepwise complete the emission reduction. And Tier 4 finial standards require that emissions of NOx and PM be further reduced by about 90% versus Tier 4 interim level. Such emission reductions can be achieved through the use of control technologies—including advanced exhaust gas after-treatment—similar to those required by the 2007-2010 standards for highway engines.

Table 3 U.S. EPA Tier 4 standards for non-road engines and equipment (g/ kWh)

Rated Power (kW)	Tier 4 Period	Year	NMHC	NMHC + NOx	NOx	PM	CO
P < 8		2008+	-	7.5	-	0.40c	8.0
8 ≤ P < 19		2008+	-	7.5	-	0.40	6.6
19 ≤ P < 37	Interim	2008-2012	-	7.5	-	0.30	5.5
	Final	2013+	-	4.7	-	0.03	5.5
37 ≤ P < 56	Interim	2008-2012	-	4.7	-	0.30	5.0
	Final	2013+	-	4.7	-	0.03	5.0
56 ≤ P < 75	Interim	2012-2013	-	4.7	-	0.02	5.0
	Final	2014+	0.19	-	0.40	0.02	5.0
75 ≤ P < 130	Interim	2012-2013	-	4.0	-	0.02	5.0
	Final	2014+	0.19	-	0.40	0.02	5.0
130 ≤ P < 225	Interim	2011-2013	-	4.0	-	0.02	3.5
	Final	2014+	0.19	-	0.40	0.02	3.5
225 ≤ P < 450	Interim	2011-2013	-	4.0	-	0.02	3.5
	Final	2014+	0.19	-	0.40	0.02	3.5
450 ≤ P < 560	Interim	2011-2013	-	4.0	-	0.02	3.5
	Final	2014+	0.19	-	0.40	0.02	3.5
560 ≤ P < 900	Interim	2011-2014	0.40	-	3.5	0.10	3.5
	Final	2015+	0.19	-	3.5	0.04l	3.5
P > 900	Interim	2011-2014	0.40	-	3.5	0.10	3.5
	Final	2015+	0.19	-	3.5	0.04l	3.5

According to EPA report, when the full inventory of older non-road engines are replaced by Tier 4 engines, annual emission reductions are estimated at 738,000 tons of NOx and 129,000 tons of PM. By 2030, 12,000 premature deaths would be prevented annually due to the implementation of the proposed standards. The estimated costs for added emission controls for the vast majority of equipment was estimated at 1-3% as a fraction of total equipment price. For example, for a 175 HP (almost 130 kW) bulldozer that costs approximately $230,000 it would cost up to $6,900 to add the advanced emission controls and to design the bulldozer to accommodate the modified engine *(9)*.

Figure 3 The demonstration for Chinese construction site (Anqing City, 2015)

Table 4 China National Standards for non-road engines and equipment (g/kWh)

Rated Power (kW)	CO	HC	NOx	NOx+HC	PM
China National Stage III, 2015 (Initially scheduled at 2013)					
P>560	3,5	---	---	6,4	0,2
130≤P≤560	3,5	---	---	4	0,2
75≤P<130	5	---	---	4	0,3
37≤P<56	5	---	---	4,7	0,4
P<37	5,5	---	---	7,5	0,6
China National Stage IV, delay (Initially scheduled at 2015)					
P>560	3,5	0,4	3,5	---	0,1
130≤P≤560	3,5	0,19	2	---	0,025
75≤P<130	5	0,19	3,3	---	0,025
56≤P<75	5	0,19	3,3	---	0,025
37≤P<75	5	---	---	4,7	0,025
P<37	5,5	---	---	7,5	0,6

Situation is sort of different in China *(16)*. China, as a large developing country, has also been actively promoting the national emission standards. For example, the Chinese National IV standard regulates the environmental impact of heavy-duty diesel engines with a limit of 3.5

g/kWh for NOx. China emission standards (see Table 4) for non-road engines are based on the European standards and the lagging is almost 10 years again. For instance, the recently implemented China National Stage IIIA non-road emission legislation on machinery with rated power from 13kW to 560 kW are PM 0.2 g/kWh and NOx 4.0 g/kWh. It has lagged nearly two generations behind other contemporaneous non-road emission regulations such as Euro IV (with limitation values on PM 0.025 g/kWh, NOx 0.4 g/kWh etc.). This lagging in emission standard results in its particular situation in China. Exhausted Gas Recirculation (EGR) always bring the cost of re-designing engine air flow system, and After-treatment System (AT) increases the prices by introducing new devices. Dodging the huge cost of system upgrading, the manufacturers trend to adopt relatively low cost technical methods to meet the loose emission limits. They choose either to improve the control strategy of the loader or to update some accessories (for example the shape of combustion chamber) to achieve a necessary reduction of pollutant.

However, there is still notable improvement in this new legislation. Compared with the stage II standard, "the Limits and measurement methods for exhaust pollutants from diesel engines of non-road mobile machinery (CHINA III, IV) (GB 20891-2014)" have set tougher emission limits, improved the measurement methods further, added the emission limit for diesel engines above 560kW as well as the measurement requirements for precious metals, and revised the technical specifications for reference diesel used for measurement. After enforcement of the updated standard, the gaseous pollutant emission level of diesel engines used for non-road mobile machinery will be cut down further. The nitrogen oxides emitted from per engine attaining national Stage III standard will be reduced by 30% to 45%, and the particulate matters emitted from per engine attaining national Stage IV standard will be reduced by 50% to 94%.

2.2 Research Objectives and Scope

The objectives of the pre-study consists three parts. First, we intend to measure construction machinery (a 5-ton wheel loader) emissions during its different operational cycles. In order to understand the performance of the wheel loader, engine bench tests and on-board tests are designed. The test results are used for sensors calibration, machinery operation analysis and, furthermore, the development of emission models. Progressively, the second objective of the study is to build a dynamic NOx emission models. A methodology for modeling emission is proposed by using data from both engine bench test and on-board.

The last one is the development of DES system in the construction area. In terms of survey loges, two construction cases are studied by simulating how these construction operations are executed. Based on the engineering features of equipment, all machine and vehicles employed in the construction site have been included in the DES simulation, and the simulation is provided to implement the designed process. Statistical results will show us how machinery cooperates with others and the time a given piece of equipment spends in each of its duty cycles.

2.3 Literature Review

2.3.1 Emission Models for Non-road Machinery

The current emission evaluations of the non-road equipment rely heavily on in-lab engine tests. In reality, the emission patterns are notably different during operations and under various working conditions *(2)*. Therefore, the primary study of this project aims to develop modeling approach for predicting detailed emissions during heavy construction operations. In particular, the pre-study focuses on modeling dynamic NOx emission for a wheel loader using real data. This part reviews the relevant studies in existing literature.

Much of the previous researches on vehicular emissions focused on modeling of road transport emissions. It has been widely recognized that the aggregated models, such as MOBILE6 *(17)*, COPERT III *(18)*, IVE *(19)*, and ARTEMIS *(20)*, have difficulties to capture dynamic emission variation, especially caused by vehicle acceleration and deceleration. Therefore, the application of aggregated models is limited for estimating emission inventories for relatively coarser spatial and temporal resolutions.

Alternatively, microscopic emission models have so far been widely accepted as a powerful tool for quantifying instantaneous emissions produced by road traffic flows in local transportation projects. In literature, microscopic models are often classified into regression-based and load-based approaches. The regression-based models usually adopt vehicle instantaneous speed and acceleration as explanatory variables. Simple linear or polynomial regression function is then used to interpret the input-to-output relationship. Typical models include EMIT and VT-Micro *(21)*. These models have the advantage of being flexible, and their application scope is also wide, but they are limited due to the lack of physical interpretation of models. Moreover, the identification of the models also requires a large amount of calibration data. On the other hand, load-based models predict emissions by simulating physical phenomena related to real emission generation in vehicle engine. Although being robust and more accurate, these models are also much more complex than regression-based models. Moreover, many parameters are required as inputs to enhance the model predicting capacity. Therefore, intermediate approach has also been adopted. For example, CMEM *(22)* simplifies the physical emission generation process by using different modular components representing physical phenomena: engine power, engine speed, air-to-fuel rate, fuel use, engine-out emission, and catalyst pass fraction. Based on the combustion conditions of engine, the model calculates the instantaneous emission while classifying the on-road working conditions into stoichiometric, cold-start, enrichment, and enleanment.

Although the majority of the previous studies investigate vehicular emissions on road, the recent research trend sees more attention towards non-road emission modeling *(23).* While the emission models for road transport may take vehicle average speed, travel distance, fuel composition and other vehicle information as inputs, it is generally quite difficult to take into account of the wide range of construction equipment types and their complex operational modes *(24)*. Therefore, the current non-road emission models mainly describe the working condition of non-road equipment by critical engine parameters, instead of using state variables of individual vehicle. Based on real-world data collected via a portable emissions measurement system (PEMS) over 1,000 vehicles, Lewis et al *(25)* presented a methodology for inventorying construction fleet emissions for different types of non-road HDD vehicles, including backhoes, wheel loaders, and motor graders. Moreover, using on-board emission data collected from three excavators by PEMS, Abolhasani et al. *(26)* shows that inter-cycle variability is important for more accurate prediction of emissions in real world. In addition, the latest EPA MOVES provides corresponding modules to estimate total or average emission and fuel consumption based on the EPA NON-ROAD model *(27)*. However, the EPA non-road model is built using different datasets collected under different conditions by the PEMS. Therefore, emission estimation based on the model is not expected to be generally accurate *(28)*.

To build the microscopic emission model of non-road machinery, especially for NOx emission, lots of studies about NOx emission models of HDD provide interesting approaches. Quérel et al. *(29)* designed a semi-physical model for the prediction of NOx emissions based on the principle of diesel engine. By distinguishing transient states of engine, they presented a burned gas temperature sub-model to improve NOx estimation accuracy both in steady state and transient operations. However, even simplifying NOx kinetic sub-model to a mean-value model, such semi-physical NOx model requires many combustion parameters, which are difficult to measure and calibrate. Singh et al. *(30)* proposed a NOx emission model using the empirical relation that is based upon the real time estimation of NOx emissions. The empirical relation is a function of engine parameters such as engine speed, engine load, intake oxygen concentration, injection quantity, timing, and fuel pressure etc. As a result, the engine-out NOx emission model represented by a linear relation with the intake oxygen concentration and other key engine operating parameters (e.g. start of injection (SOI), oxygen concentration etc.) shows a good prediction capability.

2.3.2 DES Simulation and Application

Discrete Event Simulation (DES) is a strong evaluator that is favorable for the designing of construction operations. Simulation analyses normally consist of the time and cost of construction, rates for the use of resources, waiting period, and other technical details. The outcome generally indicates the vital components of the operations that have a prospect for perfection, due to which reduction in cost or time may be possible.

However, the environmental impacts of construction processes were not taken into account in the optimization process. There is still lack of knowledge on the emission estimation for the construction operations. On the other hand, such optimization requires integration of the DES model for construction operations with the emission model that quantifies the corresponding dynamic environmental impacts *(31)*.

After examining the literature on asphalt hauling and paving operation, Lingguang et al. *(32)* describe a framework of real-time simulation for short-term scheduling, which is applicable to repetitive construction operations. They showed the whole asphalt concrete cycle consisting of the production, hauling and paving process from the perspective of the dump truck. The loading and unloading machine resources utilized in the whole process include plant, buggy and paver resource. Lau et al. *(33)* present a case study to demonstrate the impact of different operational policies on equipment idle time and operational efficiency. In their case study, the activity cycle diagram (ACD) contains the loading process that needs the heavy loaders to load soil on the dump trucks compared with the former research. A detailed description of the ACD elements is presented in Ioannou et al *(34)*. The problem Ioannou and Martinez presented describes a complex earthmoving operation for dam construction. In their simple earthmoving simulation model, there are resources in the queues LoadersWait and TrucksWait that precede it. When the process starts, it removes once resource from each of these two queues. Therefore, two more kinds of resources are introduced in this model.

3. Data Collection

3.1 Objective

In order to investigate the operation characters and emission level of the engineering machinery in China, we have conducted a serial of experiments on a Z50 wheel loader in Guangxi province from March to May 2015. Figure 4 shows the 5-ton testing wheel loader. The wheel loader, a commonly used construction machinery, has a front-mounted square wide bucket controlled by two arms to scoop up loose material from the ground, such as earth, gravel or asphalt. In the construction field, a loader is generally used to move a stockpiled material from ground level and deposit it into an awaiting dump truck or into an open trench excavation. The testing diesel engine of the 5-ton wheel loader is designed for a certified for the Chinese National Stage IIIA emission regulation.

Figure 4 Illustration of the wheel loader being tested

Table 5 Main parameters of the wheel loader

Type	Z50 wheel loader
Operation weight (kg)	16600
Bucket capacity (m3)	4.5
Rated load (kg)	5000
Max. breakout force (kN)	190
Speed at max torque (r/min)	1050 Nm @1500rpm
Emission level	Stage IIIA (NOx < 4.0 g/kWh, PM < 0.2 g/kWh)
Overall length, width, height (mm)	7794×3024×3423
Max. dumping height (mm)	3600
Max. dumping reach (mm)	1190
Boom lifting time (s)	6.8
Total Hydraulic Cycle Time (s)	$\leqslant$10
Driving speed (km/h)	Forward I 0-16 Forward II 0-38

The main parameters of the wheel loader are shown in Table 5. As mentioned in the previous chapter, to maintain relatively low cost and high fuel efficiency, instead of developing either exhausted gas recirculation (EGR) or adding after-treatment systems (AT), the loader manufacturer prefers to adjusting the control strategy of common rail direct fuel injection system and redesigning the combustion chamber in cylinders to meet the Chinese National Stage IIIA non-road requirement.

3.2 Test Equipment

There is a significant difference about the usage of engine power between on-road and non-road heavy-duty vehicles. An on-road vehicle is a mobile machine that transports people or cargo. Connected to transmission, engine output power is mainly used for driving the automobile. As a result, the motion state of a vehicle is highly relative to the effective power of engine. Furthermore, speed and acceleration of a vehicle can be used to approximate parameters, such as fuel consumption and even emission level. However, Non-road engines, also known as non-road mobile machinery, are used for purposes other than for passenger or goods transport. They cover an extremely wide range of applications. For example, a hydraulic excavator may move in a very limited distance at a construction site, but its arm attached with hydraulic cylinder deliveries most of its output power to digging process. Such difference means that tracking motion state may not amply represent the operating conditions of the non-road vehicle. And the direct observation of non-road engine conditions will clearly show how the machinery works.

The experiment has been set as two different parts. First, the diesel engine bench emission test was carried to obtain information of the loader's power source. Secondly, the on-board test was designed to simulate various working cycles of wheel loaders. Therefore, according to the test schedule, the different types of devices were respectively installed in the engine test beach and the wheel loader itself. All equipment and sensors were connected via controller area network (CAN) and required to simultaneously (sampling frequency is normalized as 5Hz) upload the measurement data into the recording device. At last, all the raw data were sorted out further stored and managed in a PostgreSQL database.

3.2.1 Equipment of Engine Bench Test

Engine bench is an automatic test system for developing, characterizing, or testing engine. An engine test bench test houses several sensors (or transducers), data acquisition features and actuators to control the engine state (see Figure 5). And sensors would measure several physical variables of interest which typically include:

- Crankshaft torque and angular velocity
- Intake air and fuel consumption rates, often detected using volumetric and/or gravimetric measurement methods
- Air-fuel ratio for the intake mixture, often detected using an exhaust gas oxygen sensor
- Environment pollutant concentrations in the exhaust gas such as carbon monoxide, different configurations of hydrocarbons and nitrogen oxides, sulfur dioxide, and particulate matter

- Temperatures and gas pressures at several locations on the engine body such as engine oil temperature, spark plug temperature, exhaust gas temperature, intake manifold pressure
- Atmospheric conditions such as temperature, pressure, and humidity

During an engine bench test, information gathered through sensors is often processed and logged through data acquisition systems. Actuators allow for attaining a desired engine state (often characterized as a unique combination of engine torque and speed). Engine bench test provides sufficient information about the engine performance under steady-state and transient conditions. While the general propose of the study is to investigate the current emission level of construction machinery in China, an elaborate bench test plan can associate researchers learn about the engine in detail, as the power source is also the emission origin of construction machinery. It also implies essential knowledge for understanding the operating characteristic of construction machinery, building reliable microscope emission models, and then estimating the emission level of a construction project.

Figure 5 Demonstration for the engine test bench: the control platform (left) and the bench measurement system (right)

A 7.8 L common rail turbo-charged diesel engine is equipped to provide power for the 5-ton wheel loader. This common rail engine (CRE) is designed to meet Chinese National Stage IIIA non-road limitation without adding any after-treatment system or using exhausted gas recirculation (EGR).

Table 6 Main parameters of the testing engine

Type	4-Stroke,Water-cooling,Inline 6-Cylinder,CRDI,TCI
Displacement (L)	7.803
Cylinder bore/Travel (mm)	112/132
Compression ratio	17.5:1
Rated power (kW)	162 kW@2000rpm
Speed at max torque (r/min)	1050 Nm @1500rpm
BSFC (g/kW.h)	≤450
Idle speed (r/min)	750±50
Ignition order	1-5-3-6-4-2
Weight (kg)	≤800
Intake type	Turbocharged, Air-to-Water, liner-cooling

To obtain the information of engine performance, an engine bench test (the bench cell was provided by Wuhan University of Technology) is carried out for a 7.8 L common rail turbo-charged diesel engine coupled with PUMA OPEA control platform and AVL AMA 4000 emission analyzer. A real-time acquisition system was connected via CAN to the engine control unit, capable of receiving and recording from ECU channels (see Figure 5). Instantaneous signals such as the engine speed, torque, fueling mass, coolant temperature etc., were recorded during the test from the ECU via the CAN bus.

3.2.2 Equipment of On-board Test

Figure 6 Demonstration for on-broad test location

The on-board data collection took place in Yulin city, China. Under the assistant of Wuhan University of Technology, a construction site was picked to ensure that the on-board test was conducted in a typical construction field. Figure 6 depicts the study area and location.

Sensors selection and installation must consider the own features of test object. For example, the sensors at the engine-out tailpipe must endure high temperature that usually rises above 300 degrees. The torque measurement device should be small enough due to the extra-limited space between the engine and transmission, which makes telemetry system sometimes become the only choice for tracking engine output torque. Moreover, measurement system response time, including the signal rising time, cannot be slower than the tested on-board sensors.

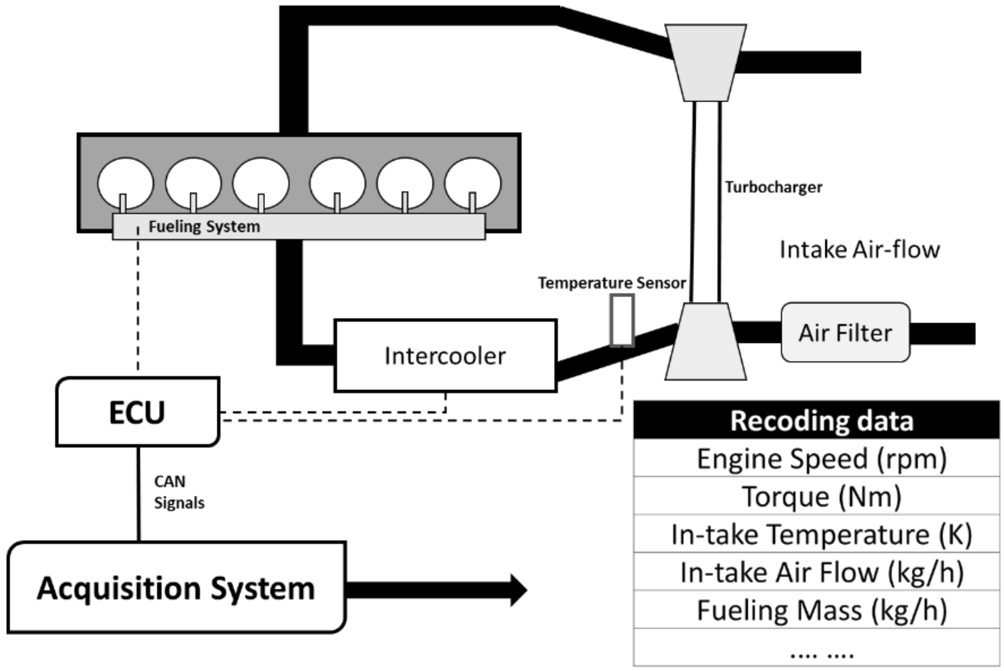

Figure 7 Demonstration for the on-board emission measurement

Table 7 Parameters of On-board Measurement

Parameters	**Sensor Type**	**Measurement Range**
Engine Speed	Magnetoelectric Tachometric Transducer	0-2500RPM
Engine Torque	TorqueTrak 10K (TT10K) Telemetry System	0- 2000 Nm
Cyclic Injection Quantity	CAN Signal from Common Rail System Signal	0-1000 mg/str
Intake Air Temperature and Pressure (both in- and out- coolant)	PT100 Temperature Sensor Pressure Transmitter	-50-200 degree & 0- 25-250kPa
Intake Air Temperature and Pressure (both in- and out- compressor)	PT100 Temperature Sensor Pressure Transmitter	-50-200 degree & 0- 25-250kPa
Exhausted Gas Temperature and Pressure (both in- and out- turbine)	PT200 Temperature Sensor Pressure Transmitter	-50-850 degree & 0- 40-500kPa
Exhausted Mass Flow	Bosch 4.2LSU Wideband UEGO Sensor	10 - 0.1 - 30 AFR*
NOx Emission	VDO Uninox24V NOx Sensor	0-2000 ppm
Environment Humidity	Hygrothermogroph	5 – 100 %
Environment Temperature	Thermometer	-50 -0.5 -120 degree

* Air fuel ratio (AFR) is based on propane Stoichiometric mixture which is 14.57

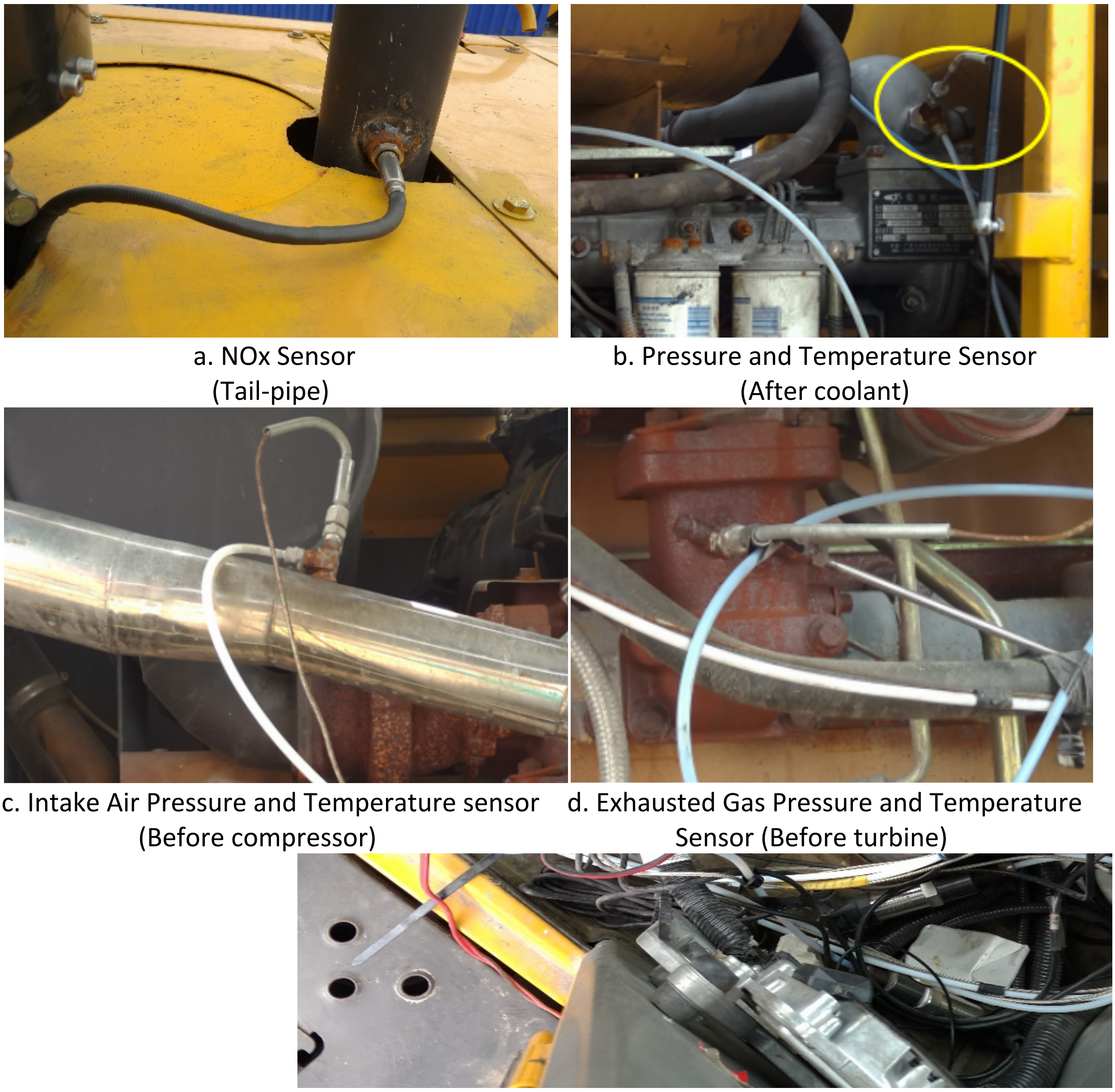

a. NOx Sensor (Tail-pipe)

b. Pressure and Temperature Sensor (After coolant)

c. Intake Air Pressure and Temperature sensor (Before compressor)

d. Exhausted Gas Pressure and Temperature Sensor (Before turbine)

e. Electronic Control Unit and Acquisition System

Figure 8 Illustration of sensors and their locations.

According to the on-board test plan, all the sensors of the acquisition system must be installed on appropriate and safe places of the loader to ensure no disturbance from equipment in various operations (see Figure 8). The parameters and the corresponding sensor types of on-board measurement are listed in table 7. The on-board data collection is based on collecting both engine and loader operational data by mechanical and electronic devices. The main specifications of these devices are shown as figure 7.

Engine speed data were measured by a hall tachometer in revolutions per minute (rpm). The torque was both mechanically measured by a linear transducer and transmitted across the engine's controlling area network as a fuel-based ECU torque signal. The mechanical torque measurement utilized rack position to determine the load being demanded of the engine. To calibrate the voltage signal from the linear actuator, the actual fuel rate, and engine-out torque, all the relevant sensors were determined based on laboratory evaluation of the same model engine. Specifically, a NOx sensor (VDO Uninox24V) was installed at the engine-out tailpipe. The sensor was carefully tested and calibrated by the emission analyzer before the on-board experiment. Since there is no after-treatment system for the wheel loader, the sensor data actually reflects the final tail-pipe emission to the air in real operations.

While considering the mechanical structure of the engine system, the delay of NOx signal should not be ignored. The reasons of NOx delay are quite complicated, including the delay of turbo charger, the time of combustion, the time of exhaust pressure wave passing, and the delay characteristics of NOx sensor etc. All of these lead to a time delay of NOx signal compared to other engine parameters. While the real delay is not constant for the non-stationary signals, a delay constant has to be empirically justified. In our data analysis, the fuel mass is selected as the reference, because the injector can instantaneously respond to the ECU order. We can observe that the total time delay between injector responses and the NOx signal parameter is around 3.7 seconds (see Figure 9).

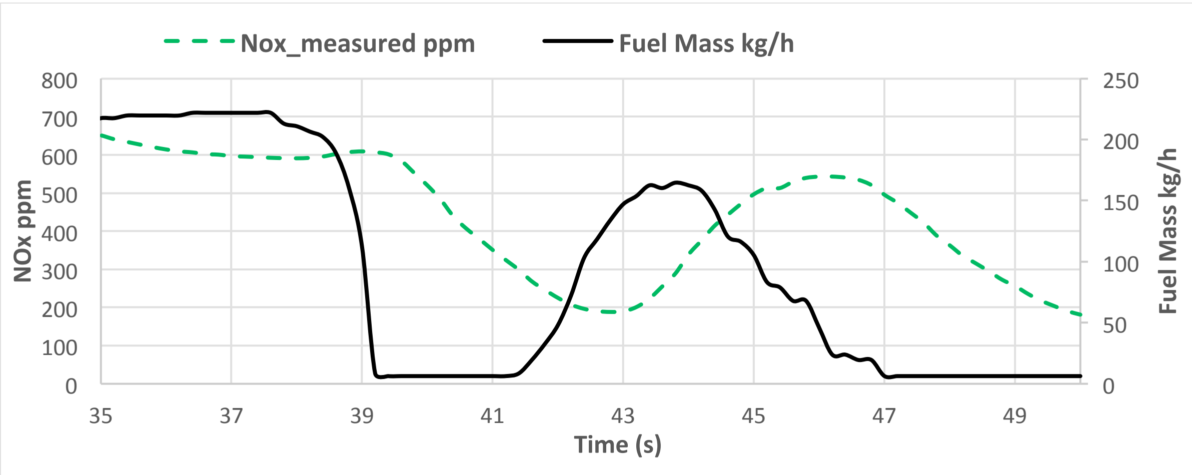

Figure 9 Demonstration of NOx delay happened in on-board measurement.

Once the calibrations of engine speed, actual torque, emission are completed, experienced operators conducted their normal work with a given test plan. The operator, who participated in the on-board tests, is familiar with the wheel loader and has more than 10 years of experience in non-road machinery operation. And the construction material in the test is the mixture of sand and gravel. The video files were also digitalized in order to extract useful information.

3.3 Test Schedule and Data Analysis

3.3.1 Engine Bench Test

The ISO 8178 is an international standard for exhaust emission measurement of non-road engines. It is wildly used for emission certification and/or type approval testing in many countries, including the United States, European Union and China. The non-road test cycles can be defined by directly reference to the ISO 8178 standard, or else by specifying a test cycle equivalent to ISO 8178 in the national legislation (as it is the case with the US EPA regulations) *(10)(11)*.

The ISO 8178 includes a collection of steady-state engine dynamometer test cycles designed for different classes of engines and equipment. Each of these cycles represents a sequence of several steady-state modes with different weighting factors. According to the ISO 8178, the China non-road current emission standard “GB20891-2014” (equivalent to EU Stage IIIA) regulates 8-mode test cycle (depicted in table 8) as the emission measurement test cycle for diesel non-road engines of 56-560 kW rated power. In particular, the 8-mode test is also referred to as the Non-Road Steady Cycle, NRSC.

Table 8 The 8-mode test cycle for non-road engine

Mode	1	2	3	4	5	6	7	8
Speed	Rated	Rated	Rated	Rated	Medium	Medium	Medium	Idle
Load	100%	75%	50%	10%	100%	75%	50%	0%
Weight	0.15	0.15	0.15	0.1	0.1	0.1	0.1	0.15

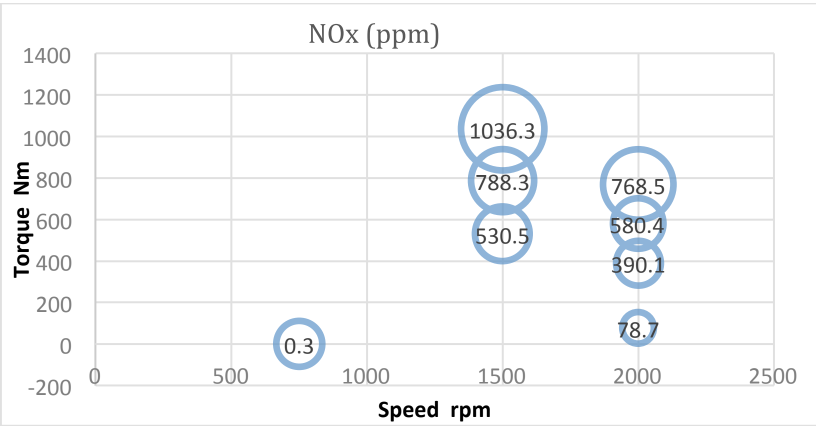

Figure 10 NOx emissions result of 8-mode test cycle

Through calculation, the results of 8-mode test cycle are: the NOx emissions 3.89 g/kWh, CH 0.047 g/kWh, and PM emissions 0.18 g/kWh. The engine performance meets the Chinese National Stage III non-road limitation. In addition to the NRSC test above, an engine performance test was designed. From the rated speed to idle speed, the length of speed step is set as 200 RPM, and similarly torque load step is 10%, down to 10% from 100%. This bench test selected about 70 steady state operating points as showed in Figure 11 below.

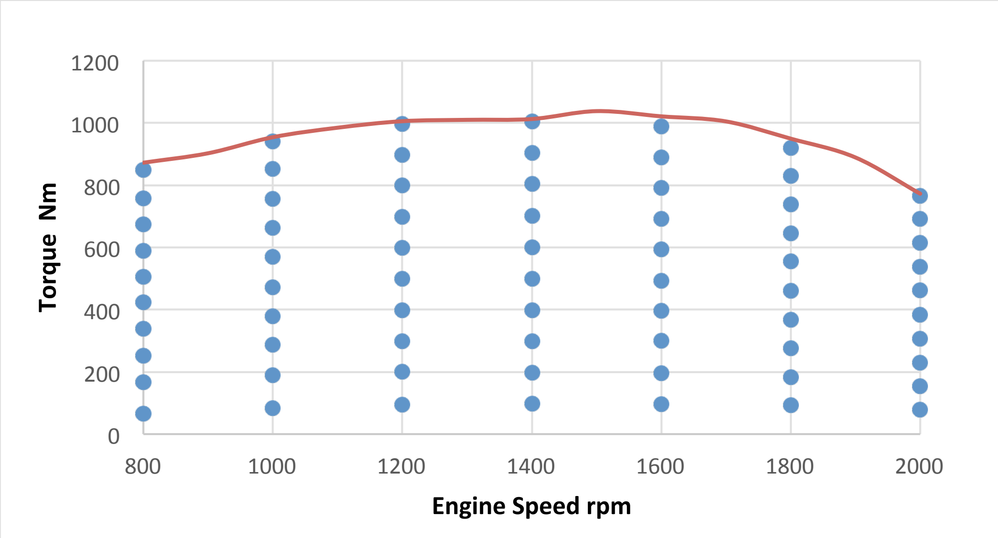

Figure 11 Engine Performance Test at 70 Steady State Operating Points

During the performance test, the AVL PUMA OPEA platform controls the variation ranges of speed and torque separately within ± 20 rpm and $\pm 2\%$ at each operating point. Covering the engine's whole operating area, the test results clearly show us its steady state characteristics. The engine parameters are recorded at each operating point, including fueling, emission value, and the gas dynamic characteristic in both intake and exhausted systems, such as pressure, temperature and mass flow.

Engine speed n and load T_q are used for locating each operating point as the x- and y-axis of each map. The rest parameters will be used to create engine and emission maps. Using quasi-stationary calculations (QS), the maps of each parameter are created based on the data measured from 70 steady state points. The bench test provided a useful way to deeply explore the reasons of why sometimes loader's performance or emission has changed unusually. It also can be compared to on-board experiment results in the next section.

3.3.2 On-Board Test

In on-board experiments, different operation modes were set to present the common operation cycles of the wheel loader: the V-cycle test, the Y-cycle test, accelerator utmost test and the driving cycle test. Based on the pre-survey at different construction sites in China, all these tests are designed for representing typical operation processes of wheel loader. For example, V-cycle is proposed as the most typical operational cycle for wheel loader, the operations of wheel load is comprised by lots of sudden transitions for the engine running. And Y-cycle appears the non-standard operational situations that are common in construction activities, especially some rural construction projects lacking of reasonable management. Accelerator utmost test shows the ultimate work task that will enforce the loader reply rising to the rated power. Such phenomenon is common in Chinese construction site when the operators want to push something beyond the maximum allowable weight. At least, the driving cycle will help us figure out the emission level of the loader at the long distance moving.

V-cycle Test

V-cycle test is designed as the typical working cycle of the wheel loader *(35)*. The shuttle back and forth operation of V-cycle is illustrated in Figure 12.

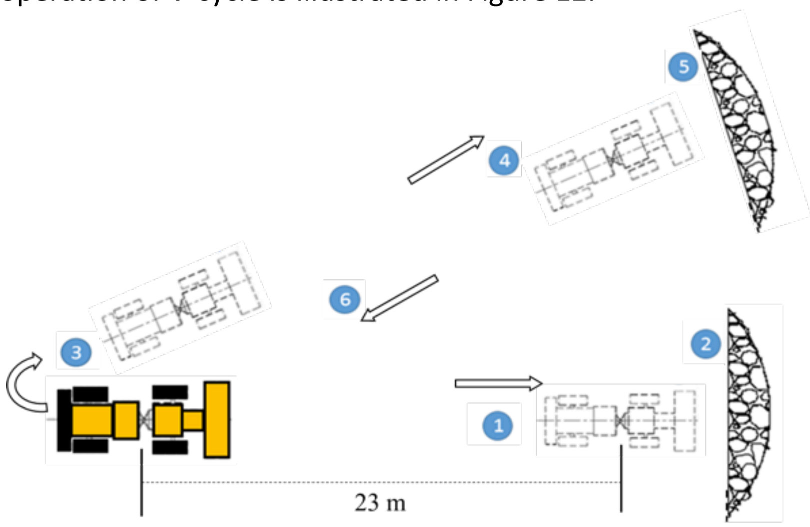

Figure 12 Illustration of the operation of V-cycle.

The operation of V-cycle includes the following six steps:

- Wheel loader is driven forward from the starting location to the material stack;
- The bucket is filled with the material;
- The loader moves backward to the starting location and steered to face the dumping place;
- The loader moves forward from the starting location to the dumping place;
- The loader dumps the material at the dumping place;
- The loader moves backward from the dumping place to the starting location.

Because the driver's operation cannot be completely consistent and standard, errors and inconsistency always existed in the operations. To ensure the data collection can reflect real operating conditions and emissions level of the wheel loader, the test time was set for 15 minutes and totally 34 times V-cycles have been done. A typical V-cycle engine operating process is intercepted from the on-board data and shown as Figure 14 below:

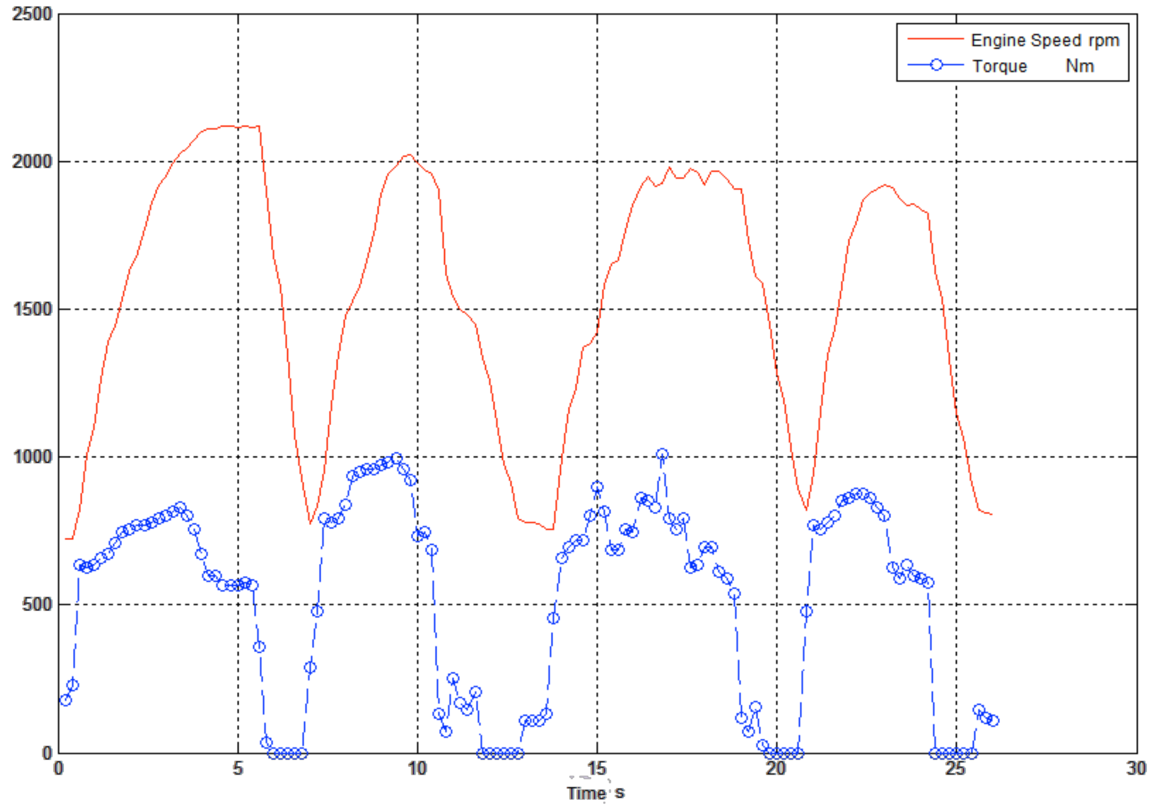

Figure 13 Illustration of the engine operating condition in one V-cycle

The road spectrum can effectively reflect the loader engine working process:

- 0 to 2 s, accelerating with empty bucket, the loader heads forward to materials stack;
- In 2-4 s, the loader slows down and closes the stack, and bucket inserts material heap by inertia;
- In 4-5 s, the joint-operation of movable arm and rocker arm filled the bucket with materials. At that time, the vehicle didn't move and the engine power output was mainly used for moving the movable arm and the rocker arm;
- In 5-11 s, the driver switched the loader to reverse gear, the loader was driven backward to the starting location with full load;
- From 11 to 15 s, the loader, carrying a full bucket of materials, accelerated to the stack;
- From 15 to 18 s, the loader moved arms, lifted the bucket, and moved the rocker arm to make the bucket discharge. Due to load changing dramatically, the engine output torque fluctuated widely;
- From 18 to 26 s, the driver switched the loader to reverse gear, and the loader backed to the starting point;

Each value of specific emissions of 34 shuttle operations in the whole I-cycle test has been different. Except for the first two cycles, all the rest cycles have exceeded 4 g/kWh, and the average of the 34 cycles is 5.3743 g/kWh. The Figure 14 demonstrates the change of each cycle.

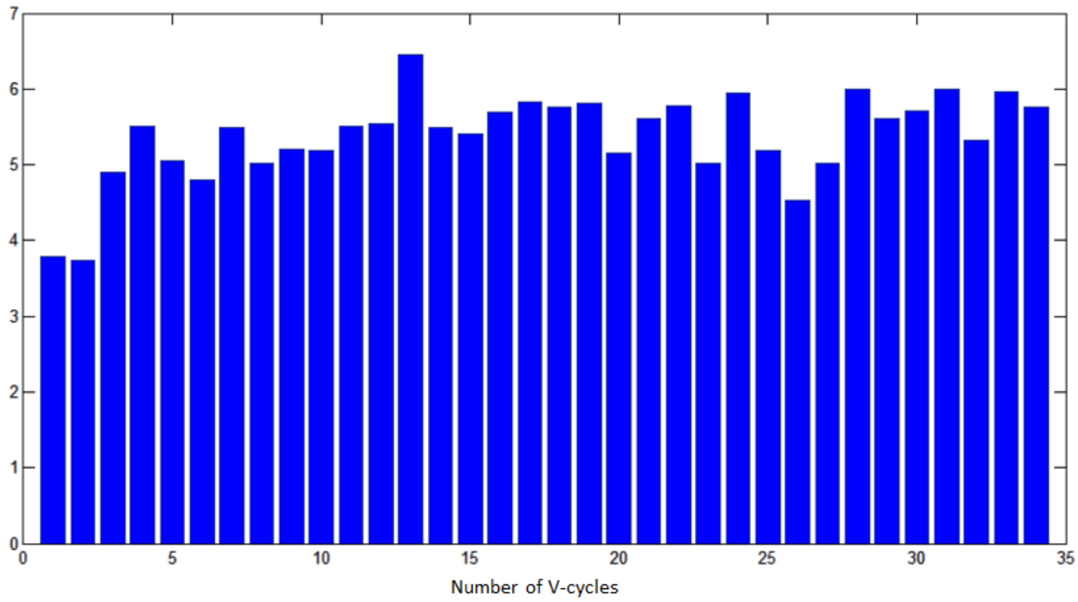

Figure 14 Specific Emissions Value in each V-cycle

According to recording data, we analyzed the test distribution of the operating process in the V-cycle test. Statistics shows that the engine mainly ran around the point of idle and the point of maximum torque (shown as Figure 15).

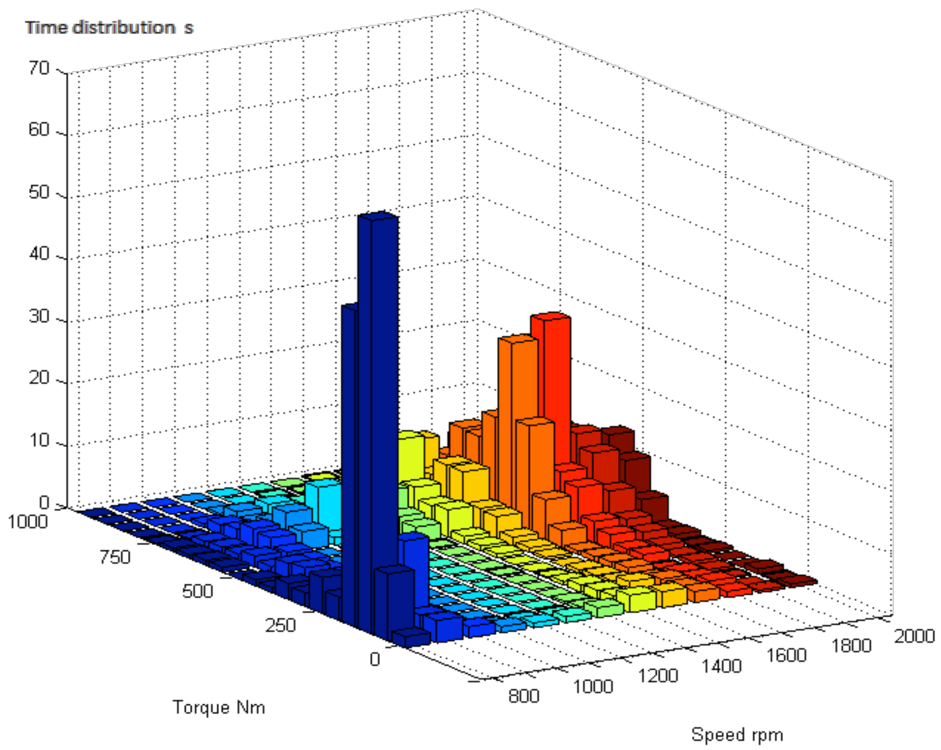

Figure 15 Time distribution of engine operational process in V-cycle test

Table 9 Distribution of working operation around idle and rated point

	Speed Range	Torque Range	Cumulative Time	Proportion
Idle Point	750-900 rpm	150-250 Nm	141.2 s	15.06%
Rated Point	1600-2000 rpm	600-1000 Nm	308.6 s	42.92%

The analysis of NOx emission indicates the NOx emission level has showed a relatively obvious coincidence with the torque. Figure 16 illustrates that the relation between NOx emission and engine torque. As mentioned in section 3.1.2, the time delay of NOx measurement is almost 3.7 sec.

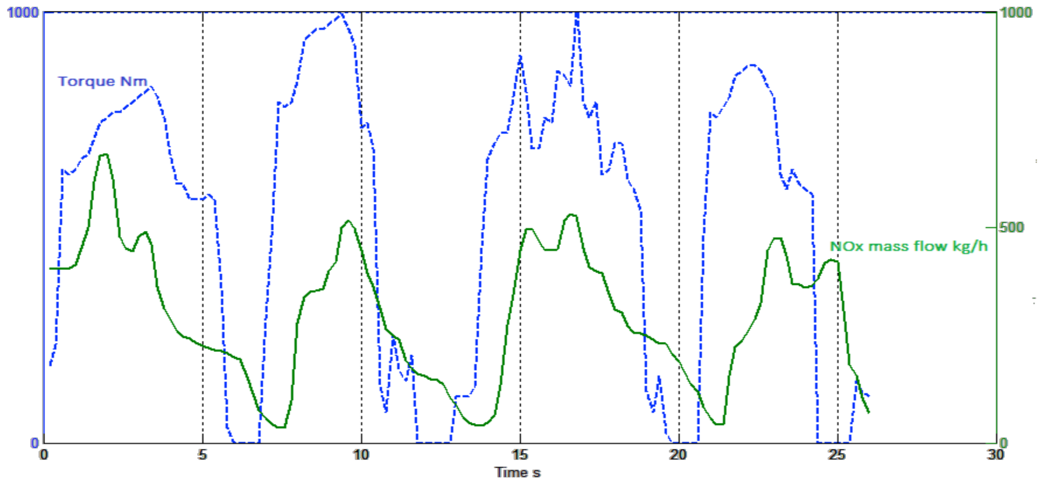

Figure 16 Torque and NOx mass flow in one V-cycle

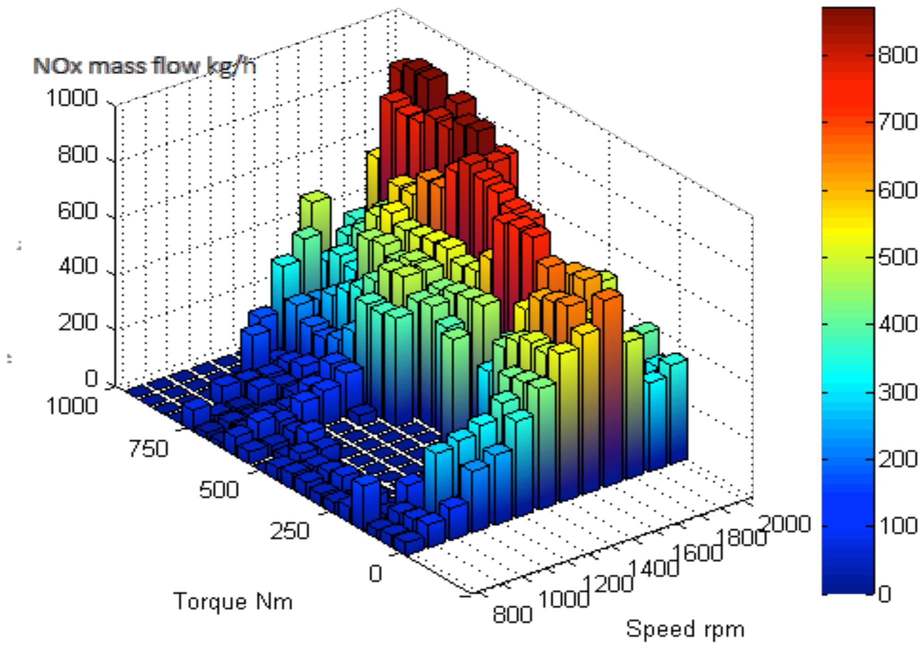

Figure 17 Distribution of NOx emission in V-cycle test

Based on the data of NOx sensor, we also got the distribution of NOx emission (see Figure 17). The value of NOx mass flow (kg/h) keeps consistent the engine speed, concerning the higher engine speed will boost larger flow and require more fueling.

Y-cycle Test

Different from the standard V-cycle, Y-cycle test in Figure 18 represents the common situation in construction. The operation cycle doesn't operate in the typical way that loader drives through straight line fast and the bucket is either full-filled or empty. In fact, the wheel loader usually chooses to operate with half-filled bucket, and the delivery route usually combines the arc way with a straight line. The Y-cycle operation has been performed repeatedly during the on-board test to simulate such operational situation. The test time was set for 15 minutes and 11 times Y-cycles have been finished.

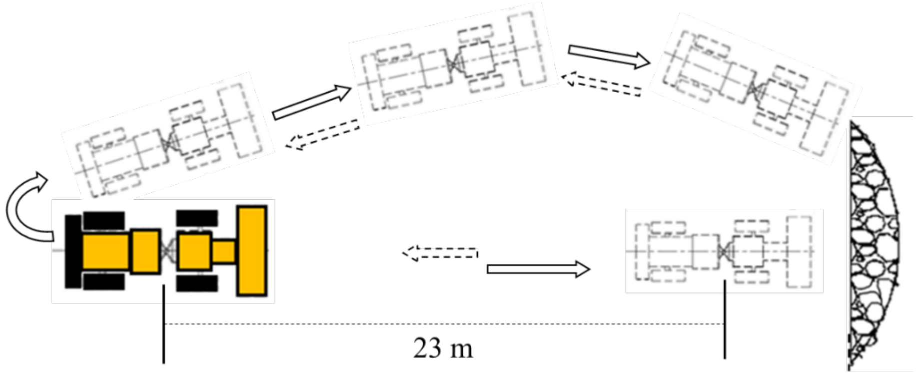

Figure 18 Illustration of the operation of Y-cycle

Similar to the steps of V-cycle, Y-cycle repeats the operating cycle of loading and dumping. However, the route of cycle and the loading requirements are totally different. Compared to the high frequency of back and forth movements of the wheel loader, the route of the Y-cycle consists an arc way and a straight line which requires the steering pump working for relative longer time. Also, the loading of each cycle is set as almost half-filled which could reflect the real-world situation. What's more, the slower driving speed and lighter loading make the engine work at low or medium load range that causes significant change on emission levels. Compared to the V-cycle, the center of Y-cycle NOx distribution moved to the medium speed area, and the lower torque significantly reduced NOx emissions. And the average of the 11 cycles is 3.933 g/kWh

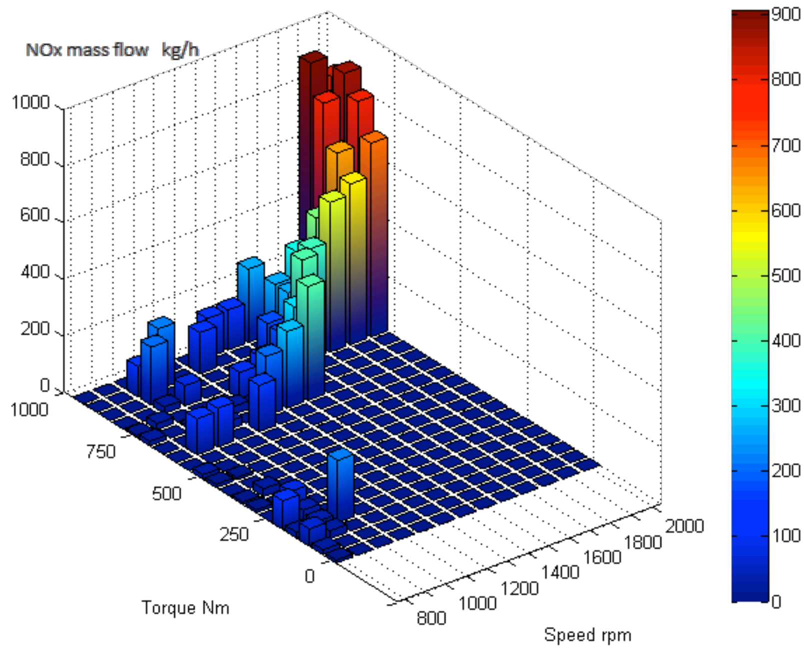

Figure 19 Illustration of NOx emission distribution in Y-cycle test

Driving-cycle Test

Considering the driving ability of the wheel loader, the driving cycle test is designed. As shown is Figure 20, the length of the driving route (blue line) is about 3 km. The Z50 wheel loader has two gears: forward I for loading and forward II for moving. Each one has its maximum driving speed. The gear of the wheel loader was set as table 10 blew that allowing the different driving speed. In addition, the road surfaces include smooth unpaved soil surface, rough gravel surface and short slopes.

Figure 20 Test route (blue lines in the map) for the driving cycle

Table 10 Results of driving test

Gear	Maximum Speed km/h	Testing speed km/h	Time s	Average engine speed rpm	Torque %	Specific NOx emission g/kWh
Forward I	12	12	963.7	2000	43	5.816
Forward II	36	20	637.6	1420	57	5.314
Forward II	36	36	365.3	2000	65	6.353

Contingent on the test results, driving cycle seems produce more NOx emission than other working cycles. Driving on the road, the loader will cause high NOx emission that is at least 1.5 times than the regulation limit.

Accelerator Utmost Test

Figure 21 Accelerator utmost Test

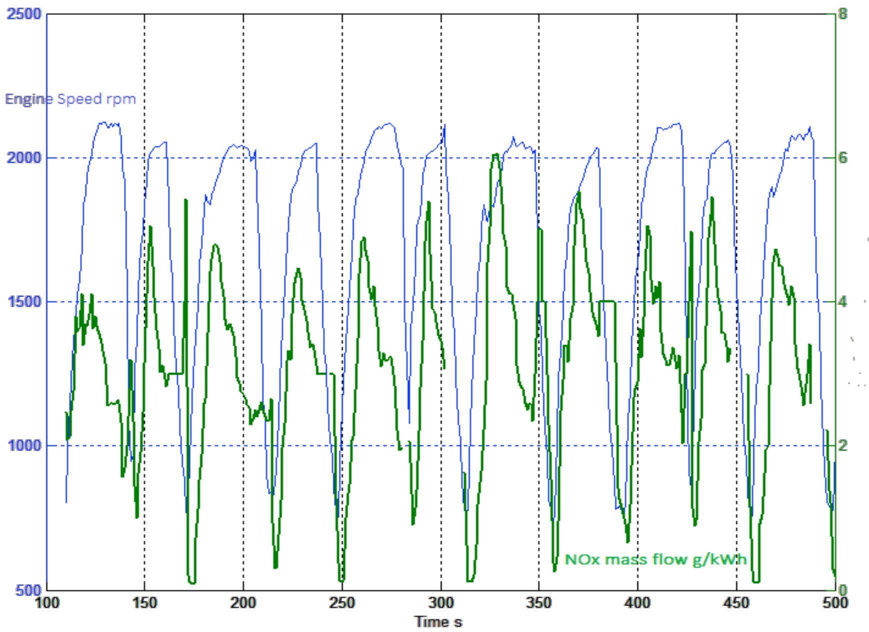

Figure 22 Demonstration for Engine speed and NOx mass flow in accelerator utmost test

As construction equipment, wheel loader often works in the ultimate state, at that time the engine will fast run around the rated point. To investigate this kind of operation, the accelerator utmost test has been designed. Before the test begins, the loader pushes its bucket into a material stack. The stack should be heavy enough, and the loader gets stuck so that it cannot furtherly move forward. At that time, the operator quickly booms the accelerator making the engine reached its rated point. The operator holds the accelerator for seconds, then loses it, and repeats such process several times until the test is over. This test can help us explore the maximum emission in engineering practice. As shown in Figure 22, the NOx maximum emission is 6.43 g/kWh, and the average result is 3.014 g/kWh.

4. Dynamic NOx Emission Model

Quantification of non-road machinery emissions will improve heavy construction process especially concerning environmental sustainability. In comparison to the substantial research effort on modeling dynamic emissions for road transport, there is however lack of knowledge on how to quantify dynamic emissions during construction operations. This section presents a load-based dynamic model for NOx emission. The model is established based on selected engine parameters that are highly correlated with the NOx generation process. In comparison to the existing approaches, the model simplifies the representation of NOx emission generation process and decomposes the complex physical processes into several modular components that correct the prediction of NOx concentration in the exhaust flow.

The data used for modeling NOx emission consists of two parts. The first one is engine bench test. It provides some fundamental information about engine performance as well as emission level. In this part, about 35 steady state points are selected on the engine state map (see Figure 11), and the engine runs at each steady state point for almost 5 minutes. The values of engine parameters at each point are measured in order to calculate maps of engine model in section 3.1. The other part is a sheet of data collected from the on-board tests. It contains signals from ECU (see Figure 7) and the instantaneous NOx emission measured by a NOx sensor. In this part, 600-second data records of the V-cycle were extracted as samples to calibrate the model coefficients in section 3.2.2. The modeling of dynamic NOx emission is based on both engine maps and correction modules, and it also needs a model to modify the NOx prediction during transient operations.

4.1 Basic Engine Map Model

As mentioned before, about 35 steady state points across the engine map are selected, and engine parameters that are recorded by acquisition system was connected with CAN to the ECU and AVL AMA 4000 emission analyzer. T parameters for building modeling maps are engine speed (n), engine load (Tq), NOx emission (NOx), intake mass flow ($\mathrm{u_{m\_int}}$), intake temperature ($\mathrm{u_{T\_int}}$), and intake temperature ($\mathrm{u_{T\_int}}$).

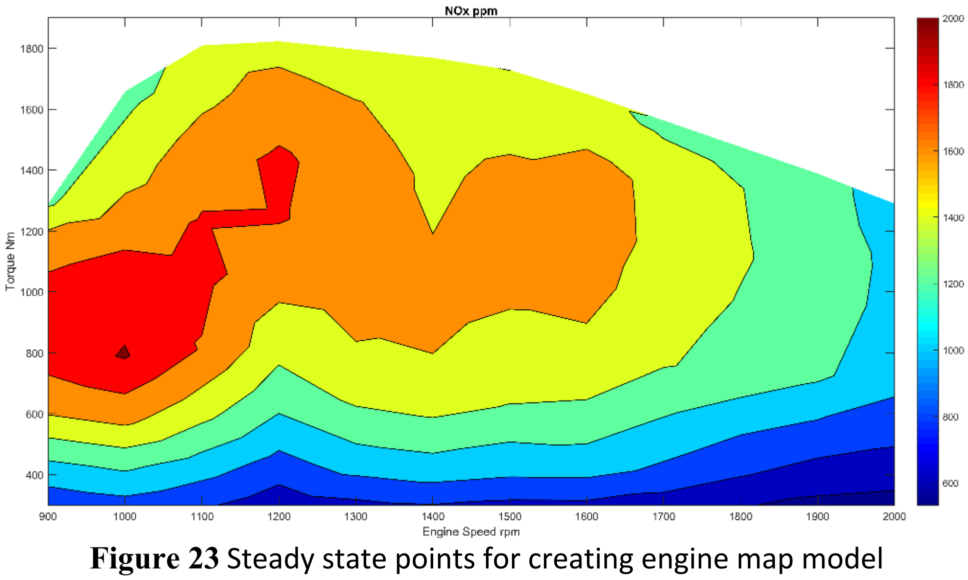

Figure 23 Steady state points for creating engine map model

Engine speed n and load Tq are used for locating each operating point as the x- and y-axis of each map. The rest of the parameters will be used to create engine and emission maps. Using quasi-stationary calculations (QS), the maps of each parameter are created based on the data measured from 35 steady state points. Specifically, the NOx maps are used to calculate the primary NOx prediction values. Similarly, other maps are respectively used to build their own correction modules for correcting the NOx predictive values.

4.2 NOx Correction Modules

As shown in Figure 24(a), NOx correction modules take three real-time signal parameters into account: in-take mass flow, in-take temperature and coolant temperature. Each correction module shares the same logic (see Figure 24(b)) and its output is the correction factor that will be multiplied by the prediction value of NOx map. Mathematically, the module function can be described by:

$$C_i(\boldsymbol{x}(t), k_i) = k_i \cdot \frac{\Delta u_i(t)}{\hat{u}_i(t)} \tag{1}$$

$$\Delta u_i(t) = u_i(t) - \hat{u}_i(t) \tag{2}$$

Where $\mathrm{C_i(x(t), k_i)}$ is the correction factor for the module i at time t, and $\mathrm{x(t)_i}$ is the instantaneous value vector of parameter i from ECU. $\mathrm{\hat{u}_i(t)}$ is the interpolation result from the corresponding parameter map created in section 4.1. $\mathrm{\Delta u_i(t)}$ describes the difference between measured value $\mathrm{u_i(t)}$ and the mapping result $\mathrm{\hat{u}_i(t)}$ of each parameter at time t. The coefficient $\mathrm{k_i}$ needs to be calibrated by the calibration dataset from the on-board test. In the modeling, 600 seconds of data selected from the V-cycle dataset is used as a typical sample of the wheel loader operational process. The basic idea of calibration is to adjust coefficient $\mathrm{k_i}$ in the each correction module to fulfill least square error (LSE) concerning the deviation between NOx prediction and measurements. Analytically, this can be represented by a non-linear optimization problem i.e.

$$\min \Phi(\boldsymbol{k}) = \sum\nolimits_{\Omega}(y(t) - \hat{y}(\boldsymbol{x}(t), \boldsymbol{k}))^2 \tag{3}$$

$$\hat{y}_0(\boldsymbol{x}(t), \boldsymbol{k}) = \hat{f}_{map}\left(n(t), T_q(t)\right) \cdot \prod\nolimits_{i=1}^{N} C_i(\boldsymbol{x}(t), k_i) \tag{4}$$

Where $\mathrm{y(t)}$ and $\mathrm{\hat{y}_0(x(t), k)}$ represent the NOx measurement and model prediction respectively. $\mathrm{x(t)}$ represents the vector of the ECU input signals in the sample space Ω. $\mathrm{\hat{f}_{map}}$ is the output of the NOx map based on the current engine speed $\mathrm{n(t)}$ and torque $\mathrm{T_q(t)}$. As mentioned before, $\mathrm{C_i(x(t), k_i)}$ is the correction factors and in this case the number of correction modules is $\mathrm{N} = 3$. And $\mathrm{k} = [\mathrm{k_{m\_int}}\ \ \mathrm{k_{T\_int}}\ \ \mathrm{k_{T\_cool}}]^{\mathrm{T}}$ is a vector of coefficients that need to be calibrated. The formulation of the problem has been implemented in Matlab/Simulink. The Optimization Toolbox is used. The optimized coefficients vector is shown in table 11 below.

TABLE 11: Parameters for correction modules in the NOx correction subsystem

Correction Module	i	Correction factor C_i	Coefficient k_i	Optimized k_i
Intake Mass Flow	1	C_{m_int}	k_{m_int}	0.329
Intake Temperature	2	C_{T_int}	k_{T_int}	0.781
Coolant Temperature	3	C_{T_cool}	k_{T_cool}	0.505

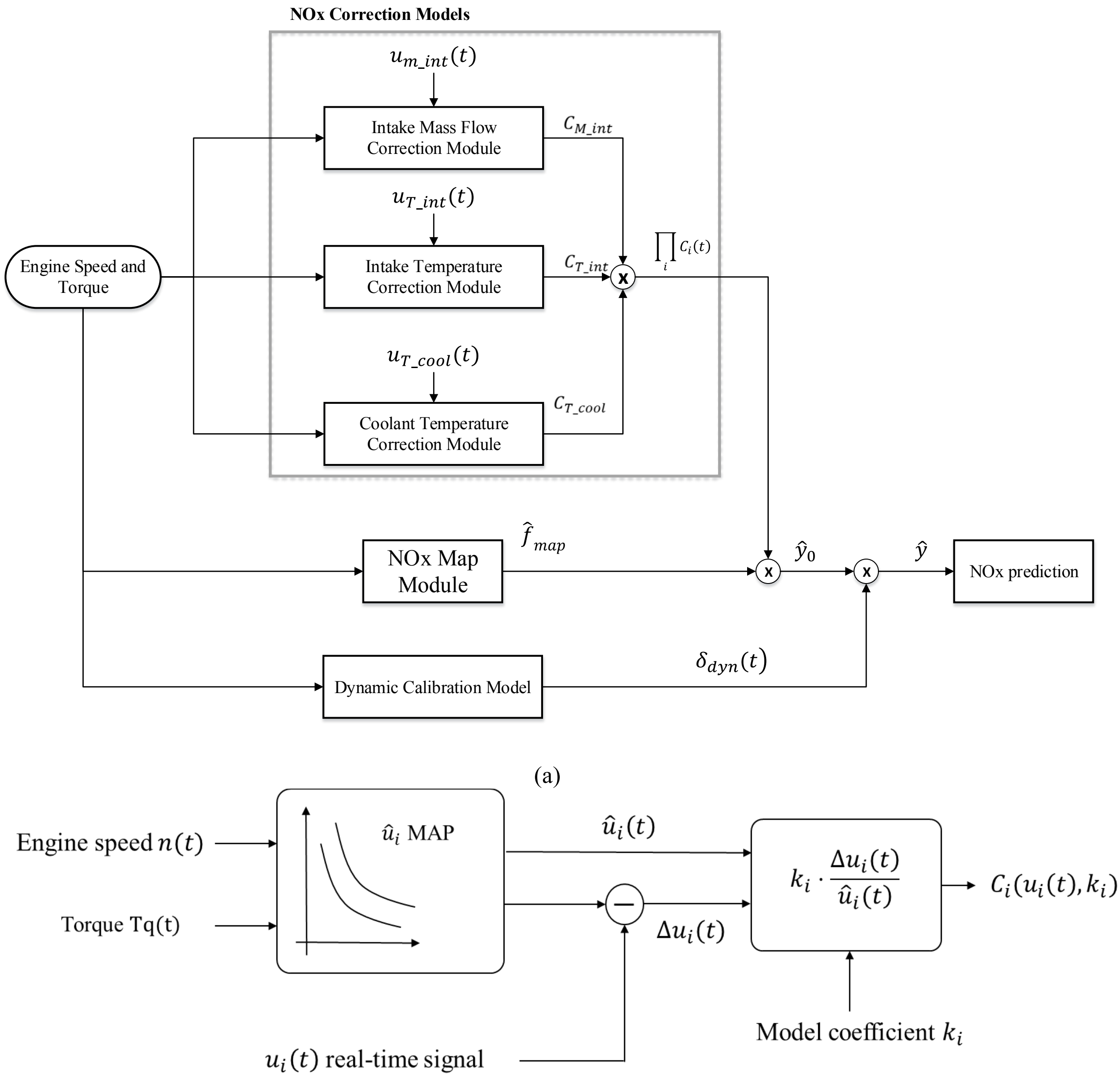

(b)

Figure 24: the architecture of the NOx emission model (a) and the diagram to demonstrate the principle of the correction module (b).

4.3 Dynamic Calibration Model

Since the operations of wheel loader includes transitions of high frequency among different engine states, the emission measured on-board may fluctuate abruptly in a wide range. This characteristic augments the difficulty to accurately predict the NOx emission in dynamic operations. Figure 4a shows that there is still relatively large deviation between NOx measurement and prediction after the correction module. Therefore, a model is added to improve the model accuracy in Figure 4b. In this model, the change ratios of engine speed Δn and torque and ΔT_q were chosen to express how fast the change of operational state happens.

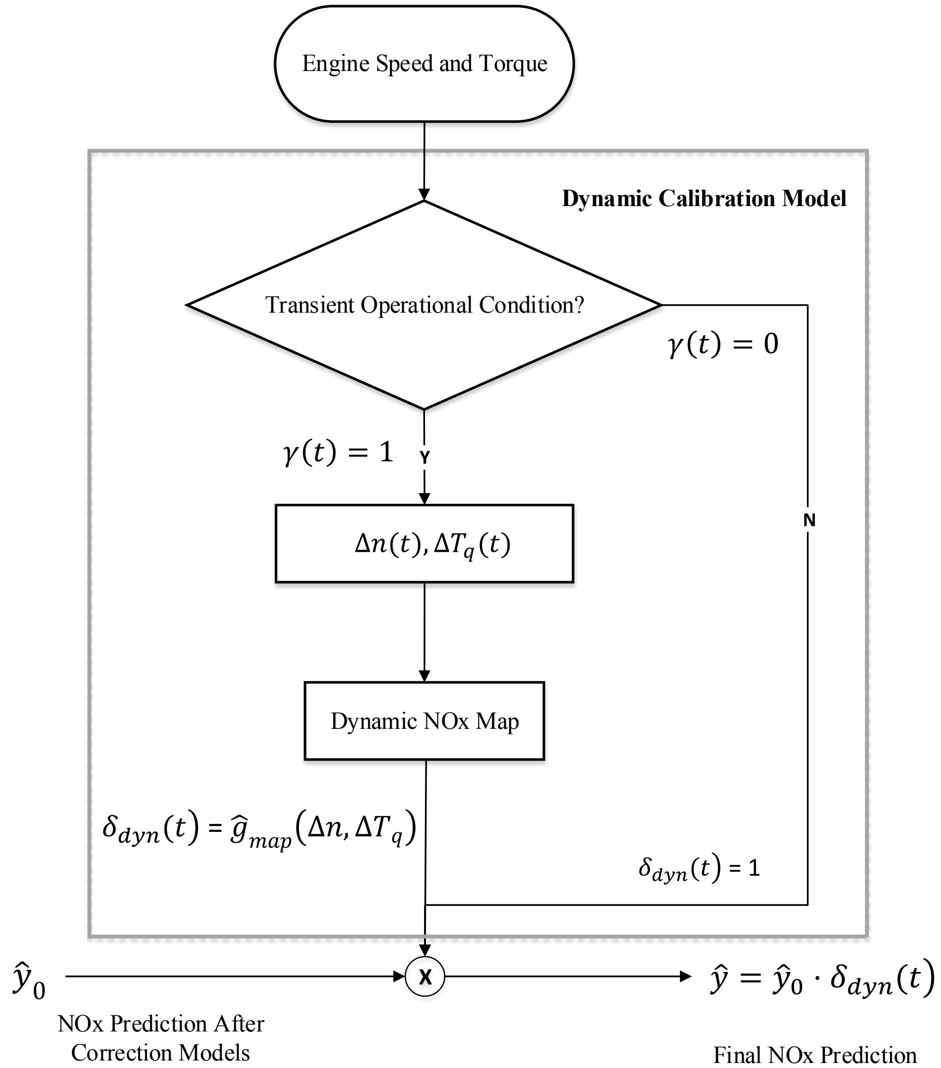

Figure 25: A diagram illustrating the working principle of the dynamic calibration model.

Figure 25 illustrates how the model works. The first step is to distinguish whether the current engine condition belongs to transient operational condition through the signals of engine speed and torque. The signals are recorded for 8 seconds before the current time are used to justify the condition. Then the algorithm of the model simultaneously averages them to be $\overline{\mathrm{n}}$ and $\overline{\mathrm{T_q}}$. If any of the recorded speed or torque data exceeds the upper or lower bound calculated by multiplying $\overline{\mathrm{n}}$ or $\overline{\mathrm{T_q}}$ with $\pm 120\%$, it will consider the current condition as a transient operation.

A binary variable $\gamma(\mathrm{t})$ was set to present whether or not the condition is transient. According to the values of $\Delta\mathrm{n}$ and $\Delta\mathrm{T_q}$, the algorithm will refer the dynamic map and outputs the factor named as $\delta_{dyn}(t)$. Otherwise, the whole dynamic calibration model will not affect the NOx prediction the factor i.e. $\delta_{dyn}(t) = 1$. The final prediction values of NOx model are the results of previous NOx prediction multiplying the factor $\delta_{dyn}(t)$, as given by the formulas (6) and (7).

$$\hat{y}(\boldsymbol{x}(t), \boldsymbol{k}) = \hat{f}_{map}\left(n(t), T_q(t)\right) \cdot \prod_{i=1}^{n} C_i(\boldsymbol{x}(t), k_i) \cdot \delta_{dyn}(t) \quad (6)$$

$$\delta_{dyn}(t) = \begin{cases} \hat{g}_{map}(\Delta n, \Delta T_q) & if \quad \gamma(t) = 1 \\ 1 & else \quad \gamma(t) = 0 \end{cases} \quad (7)$$

Where $\hat{g}_{map}(\Delta n, \Delta T_q)$ donates the result of the dynamic map indexed by Δn and ΔT_q, $\hat{y}(x(t), k)$ is the final prediction values at t time, with the instantaneous inputs $x(t)$ and the optimized coefficients vector k.

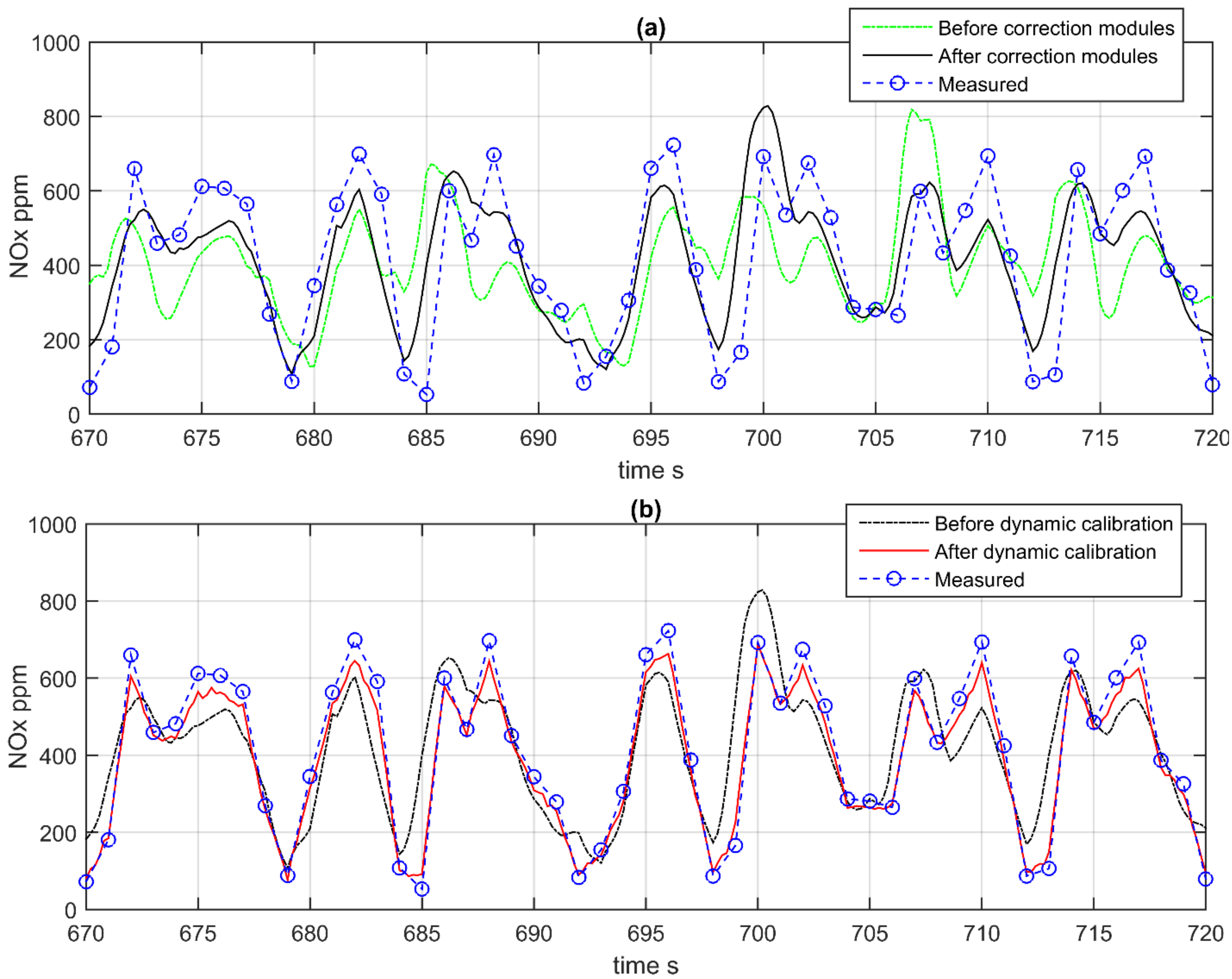

Figure 26: Comparison of the model performance: before and after applying correction modules (a); before and after applying dynamic calibration model (b).

4.4 Model Validation

After the calibration using random selected data during operation in Y-cycle, it is essential to verify prediction performance of NOx models using out-of-sample data. We verify the accuracy and reliability of the NOx emission model by comparing with the results measured from the three different cycles that the wheel loader was tested. Several statistical measures are calculated for evaluation of model performance *(36)*, including root mean square error (RMSE) and mean absolute percentage error (MAPE).

The RMSE is estimated by

$$\mathrm{RMSE} = \sqrt{\sum_{i=1}^{N}(E_i - \widehat{E_i})^2/N} \tag{8}$$

Where E_i is the NOx data obtained from the on-board emission experiments, $\widehat{E_i}$ is the emission model prediction, and N is the size of samples. The MAPE index is computed by:

$$\mathrm{MAPE} = \sum_{i=1}^{N}\left|E_i - \widehat{E_i}\right| / \sum_{i=1}^{N} E_i. \tag{9}$$

TABLE 12: Evaluation of the model performance

		NOx Map		**NOx Map with correction modules**		**Final NOx Model**	
Test modes	Data size (s)	RMSE (ppm)	MAPE (%)	RMSE (ppm)	MAPE (%)	RMSE (ppm)	MAPE (%)
V-cycle	2100	240.32	37.15	114.7	21.43	71.22	17.25
Y-cycle	1620	189.27	43.21	154.73	34.64	110.43	29.52
Driving cycle	730	120.43	59.57	101.25	28.91	96.29	23.81

Table 12 shows the model validation results using out-of-sample NOx emission time series data sets measured from three on-board test cycles. The final NOx model in Table 12 is the final prediction value of NOx model, which has been modified by both correction and dynamic calibration models. Correction modules can generally improve the accuracy of prediction. The validation results show that the introduction of correction modules largely reduces the value of MAPE corresponding to each test cycle and the lowest RMSE is achieved after the processing by the dynamic calibration model.

As a result, the final NOx model could accurately predict the trends of on-board emission signal. Especially, the performance is pretty good when the engine state changes frequently and emission fluctuates abruptly in a wider range.

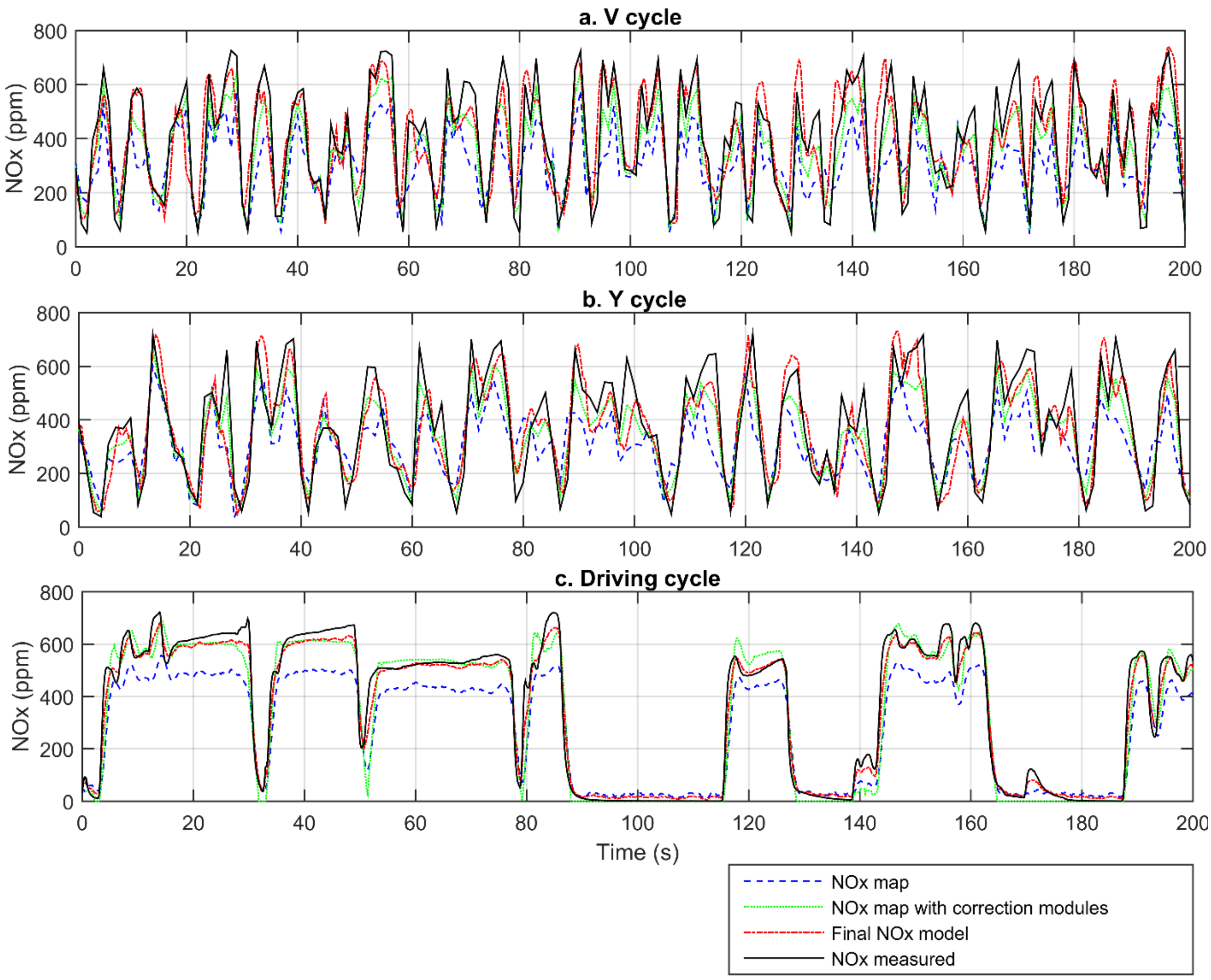

Figure 27: An example of the dynamic NOx model validation.

Being the most typical operational cycle for wheel loader, the operations in V-cycle contain lots of sudden transitions for the engine working condition. The NOx model seems able to handle the transient condition well (see Figure 27(a)). Different from the V-cycle, Y-cycle shows the non-standard operational conditions that are common among construction activities, especially some rural construction projects lacking of reasonable management (see Figure 27(b)). In fact, on-board test data shows that Y-cycle allows the engine working at totally different conditions. When the wheel loader is set as forward II and driving at the speed of 25km/h, the model results are also reliable (see Figure 27(c)). Compared to the NOx map that has been widely used to quantify instantaneous emission, the proposed NOx model shows obviously better prediction performance in the validation of all the test cycles.

4.5 Summary

Modeling non-road emission is essential for management of pollutant emissions generated during heavy construction projects. This paper develops a dynamic NOx emission model using on-board measurement data collected by a wheel loader in the Chinese operational environment. Instead of focusing on non-road equipment that potentially may have big differences between each other, this modeling study mainly considers engine state and operational condition, which is an effective approach for handling the inconsistency in different mechanical categories and working cycles.

The on-board NOx emission is measured together with all engine parameters. A NOx emission map model is initially established from the data collected during the engine bench test. Then data randomly selected from on-board measurement during V-cycle is applied to calibrate the NOx model by two modules. The model parameters of the correction module are optimized by searching for the least square prediction error. The sample data is also used to create dynamic map for building the dynamic calibration model used to identify transient operations and then improve model prediction. The model is finally validated using out-of-sample NOx emission time series from three different cycles. While the model shows best performance in predicting emission in Y-cycle, the validation results with the other two cycles show also good performance. In addition, the analysis shows that both the correction and dynamic calibration models are essential for the improvement of the model performance.

5. DES Simulation on Construction

Discrete event simulation has been widely used to model and evaluate engineering systems and has been an on-going area of research and development *(37)*. Discrete-event simulation (DES) in the construction industry can be found in the planning and optimization of construction operations that are repetitive in nature in earthmoving, tunneling, sewer-line construction, and paving operations in heavy construction projects. Controlling the emissions of all construction machinery in the construction project is a critical step in the environmental management of construction processes. The operational characteristic of construction projects has motivated research and practical applications of discrete-event simulation (DES) in the construction industry.

The DES simulation focuses on modeling interaction between different construction machinery during construction operations. Based on the engineering features of equipment, all machine and vehicles employed in the construction site have been defined as a unit, and the simulation is provided to implement the designed process. The process-based discrete-event simulation framework 'Simpy' is used to edit different processes and simulate the situation. The ambition of this study is to simulate the processed that are operated by each unit.

5.1 Case Study 1: CAP Case

The central asphalt plant (CAP) is the location where the hot-mix asphalt is normally produced. A double-barrel drum mix process including blending, heating and mixing aggregates and asphalt cement is completed here. Additionally, the plant produces a continuous flow of asphalt concrete. Fresh asphalt concrete is stored in the storage silos from which it can then be dispatched into dump trucks by heavy front-end loaders. Dump trucks at the loading area queue up and are loaded in FIFO order. Each dump truck is loaded by one loader once a time. When a dump truck is loaded it starts hauling the asphalt concrete to the work zone.

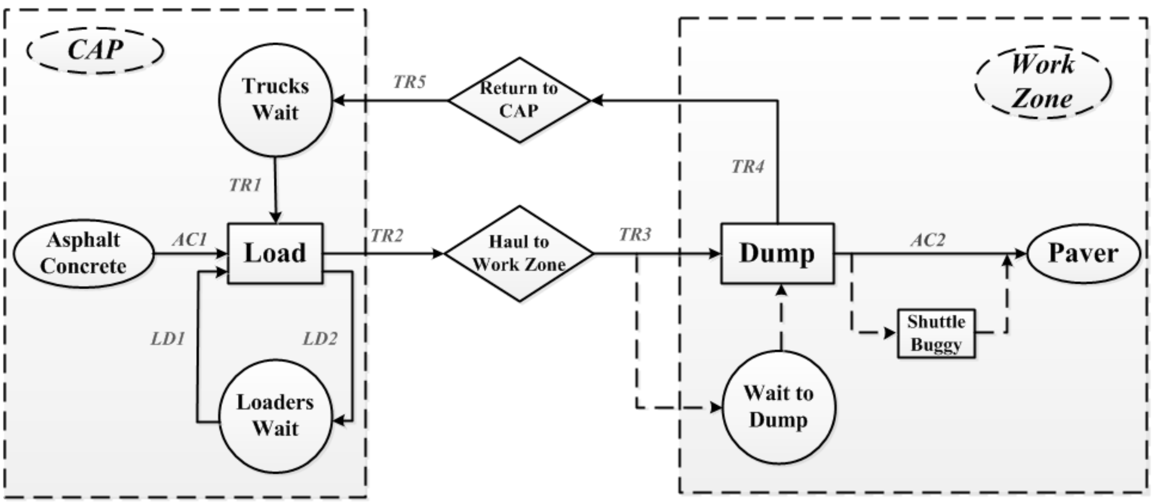

Figure 28 Demonstration for construction process

After entering the work zone, dump trucks discharge the asphalt concrete into a shuttle buggy that is a material transfer vehicle (MTV) transferring the asphalt concrete from dump trucks to the paver. The shuttle buggy gets its asphalt from the dump trucks and keeps the paver supplied with hot asphalt mix. When paver is uploaded with asphalt concrete, it starts paving. A simple simulation is provided to implement the designed process. The purpose of this study is to simulate the process moving the asphalt concrete from the central asphalt plant to the work zone. The loading and hauling operations rely strongly on heavy equipment so that we make use of 'Volvo L60G' loader (38) and 'Volvo A25D' dump truck (39) for simulation. The basic parameters of dump truck and loader are as table 13 and table 14.

Table 13 Volvo A25D (dump truck)

Parameters	Value
Load Capacity SAE 2:1 heaped	15 m3
Payload	24 000 kg
Max Speed	53 km/h
Gross Weight	45.6 t
Body Raise Time	12 sec
Body Lower Time	10 sec

Table 14 Volvo L60G (loader)

Parameters	Value
Bucket Capacity	1.91 m3
Travel Speed	8.05 km/h
Digging Depth	4.1 inches
Raise Time	4.5 sec
Dump Time	2.3 sec
Operating Load	7.610 lbs
Tipping Load	18.070 lbs

5.1.1 Set Up

We set up a construction case that includes three main processes. The dump truck is firstly loaded asphalt concrete at the central asphalt plant by heavy loaders. Then, it starts driving from the central asphalt plant to the work zone when it completes loading procedure. The final process is to dump the asphalt concrete to the shuttle buggy in the work zone and then the truck returns to the central asphalt plant, after which the next cycle is about to start.

Table 15 Value of variables

Variables	Value
The number of loader	2
The number of buggy	1
The number of truck	4
Loading Time	1 min
Unloading Time	1.5 min

In the case study, the value of some variables has been given. The number of loaders that are provided in the central asphalt plant (CAP) is two and there is only one available shuttle buggy in work zone for unloading. The loading time that is spent to load a dump truck is (4.5+2.3)*15/1.91=53.4 sec and we assume the loading time obeys the normal distribution (μ=1 min, σ^2 = 0.1). In the work zone, the dump truck need some time (12+10=22 sec) for raising and lowering its body. It costs approximately 1 minute to dump the asphalt concrete to the shuttle buggy so that we assume that the value of unloading time obeys the normal distribution (μ =1.5 min, , σ^2=0.15). In addition, we create 4 dump trucks that are at the central asphalt plant when the simulation starts.

Besides, two driving processes are generated including the one from central asphalt plant to work zone and from work zone to central asphalt plant. The driving time obeys normal distribution where the mean value is 5 (minutes) and the standard deviation is 0.5. Therefore, we generate some random numbers, each for a dump truck driving process.

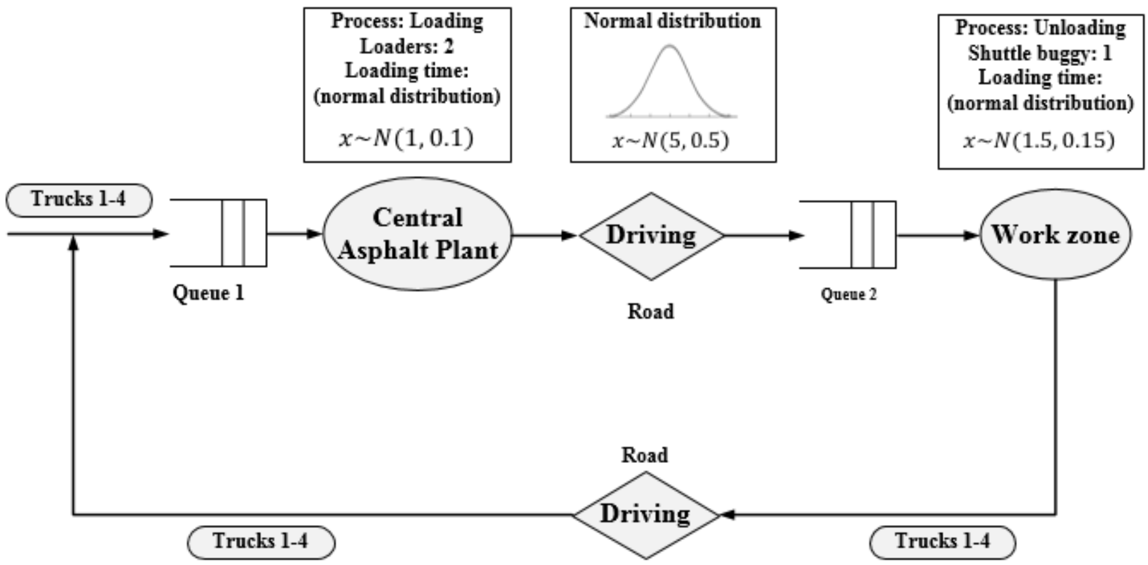

Figure 29 Simulation process for CAP case study (unit: min)

5.1.2 Simulation Results

In the simulation process, we set up the simulation time as 60 minutes and run the simulation. Then, we show the construction processes of the first two cycles as below. For example, in the beginning, four trucks arrive at central asphalt plant at the same time (0.00 sec). But only truck 1 and 2 enter and start loading process. Truck 3 and 4 wait until truck 1 and 2 leave (1.00 sec) and then they enter and start loading. We also find that the time truck 4 leaves central asphalt plant is at 2.00 sec and the truck 1 returns to central asphalt plant at 12.94 sec. Therefore, these two loaders experience the waiting process from 2.00 sec to 12.94 sec. In addition, buggy in the work zone is also idling sometimes, such as: the periods from 0.00 sec to 5.70 sec and from 11.70 sec to 18.88 sec.

Table 16 Construction process of truck 1

Truck id	Area	Action	Time (s)
1	Cap	Arrive	0.00
1	Cap	Enter	0.00
1	Cap	Leave	1.00
1	Work zone	Arrive	5.70
1	Work zone	Enter	5.70
1	Work zone	Leave	7.20
1	Cap	Arrive	12.94
1	Cap	Enter	12.94
1	Cap	Leave	13.94
1	Work zone	Arrive	18.88
1	Work zone	Enter	18.88
1	Work zone	Leave	20.38

Table 17 Construction process of truck 2

Truck id	Area	Action	Time (s)
2	Cap	Arrive	0.00
2	Cap	Enter	0.00
2	Cap	Leave	1.00
2	Work zone	Arrive	6.12
2	Work zone	Enter	7.20
2	Work zone	Leave	8.70
2	Cap	Arrive	13.69
2	Cap	Enter	13.69
2	Cap	Leave	14.69
2	Work zone	Arrive	19.13
2	Work zone	Enter	20.38
2	Work zone	Leave	21.88

Table 18 Construction process of truck 3

Truck id	Area	Action	Time (s)
3	Cap	Arrive	0.00
3	Cap	Enter	1.00
3	Cap	Leave	2.00
3	Work zone	Arrive	7.00
3	Work zone	Enter	10.20
3	Work zone	Leave	11.70
3	Cap	Arrive	16.61
3	Cap	Enter	16.61
3	Cap	Leave	17.61
3	Work zone	Arrive	23.61
3	Work zone	Enter	23.61
3	Work zone	Leave	25.11

Table 19 Construction process of truck 4

Truck id	Area	Action	Time (s)
4	Cap	Arrive	0.00
4	Cap	Enter	1.00
4	Cap	Leave	2.00
4	Work zone	Arrive	6.62
4	Work zone	Enter	8.70
4	Work zone	Leave	10.20
4	Cap	Arrive	15.04
4	Cap	Enter	15.04
4	Cap	Leave	16.04
4	Work zone	Arrive	20.56
4	Work zone	Enter	21.88
4	Work zone	Leave	23.38

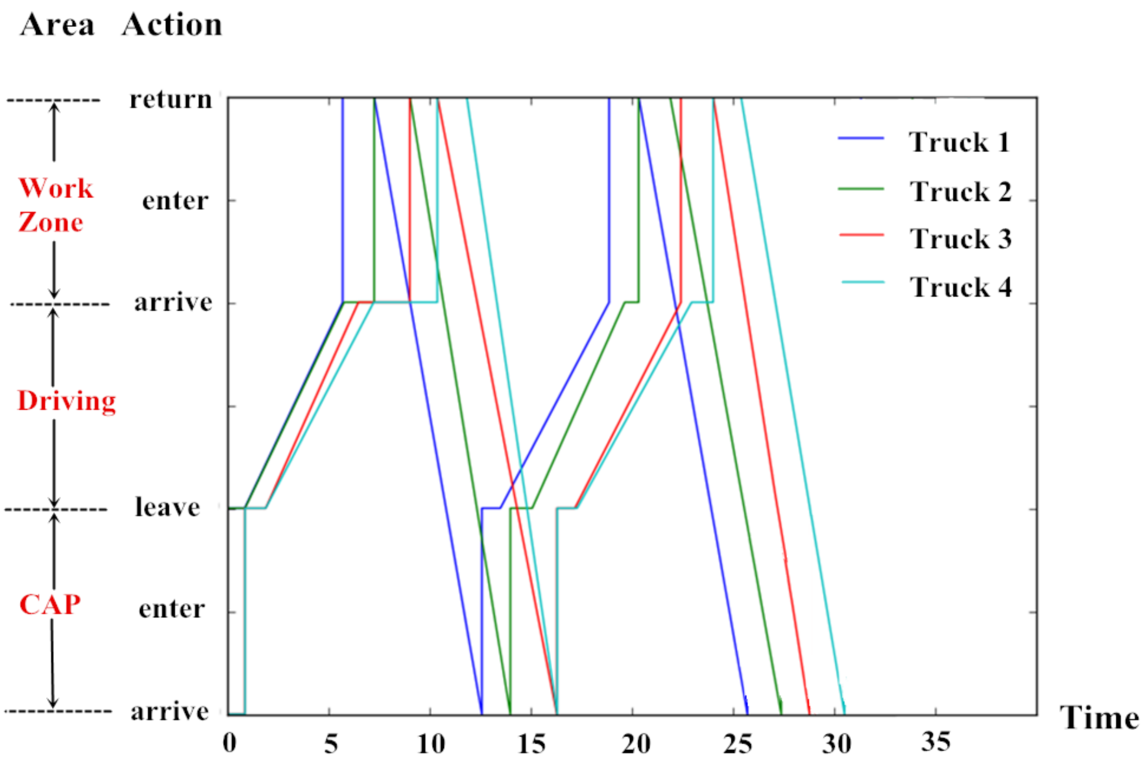

Figure 30 The DES results of trucks trajectory

Besides, figure 30 shows the truck moving trajectory in the first two cycles. We can see the four trucks arrive at the CAP when the simulation begins. Because of the limitation of the number of loader only first two trucks can start loading at the very beginning. Then, the latter two trucks enter the loading area when the loaders are available. Actions happened in work zone are more complicated since there is only one shuttle buggy used in the unloading process. Trucks arrive at the work zone and wait to enter until the former truck leaves. The waiting time can be easily observed from the length of horizontal lines.

5.2 Case Study 2: Earthmoving

Earthworks are a common early stage part of heavy construction engineering and involve the digging, moving and dumping of the soil from the construction site *(40)*. Case 2 is based on the survey about earthmoving operations happening in a construction site in China. Figure 31-32 illustrates the earthmoving operations during our survey in Anqing city, China.

Figure 31 Loading stations in the construction site

Three excavators crushed earth and loaded on dump trucks at the different loading stations in the construction site (see Figure 31), and about 8 dump trucks were commuting between the construction site and the dumping zone for delivering crushed earth. The distance between these two places is 6.7 km. Subjected to the local regulations, the haul trip and the return trip were on different route, and the average time of these two trips are 9’12’’ and 12’35’’, respectively. The operations of the earthmoving can be described as following:

1. The excavator uses its arm to consistently dig and load the earth on the waiting dump trucks (see Figure 31);
2. After fully filled, the dump truck leaves the loading station and another truck enters the loading station;
3. According to the local environmental regulations, the dump truck needs to be totally washed and checked before it drives into the high way (see Figure 32).
4. After arriving at the dumping zone, the truck may have to wait in the line because there is only two dumping port at this zone.
5. After dumping and washing, the truck returns to the loading station for another load-and-haul cycle.

Figure 32 Washing the dump truck before it leaving the construction site

There were three excavators used at the loading stations: one 'Volvo EC140B Prime' and two 'HITACHI ZX200-3' excavators. And 8 'Sinotruk ZZ3257' trucks cycled between construction site and dumping zone. The max-load of 'Sinotruk ZZ3257' trucks is 30t (although overloading always happens). The basic parameters of dump truck and excavators are listed in the tables below.

Table 20 Sinotruk ZZ3257 (dump truck)

Parameters	Value
Load Capacity	20 m3
Max Payload	30 000 kg
Max Speed	75 km/h
Gross Weight	32 t
Engine Power	250 kW
Fuel Consumption	196 g/kWh
Emission Level	Euro 2

Table 21 HITACHI ZX200-3 (excavator 1)

Parameters	Value
Bucket Capacity	0.9 m^3
Engine Power	122 kW
Digging Depth	6.6 m
Digging Reach	9.2 m
Operating Weight	20.2 t
Emission Level	EU Stage III

Table 22 Volvo EC140B Prime (excavator 2)

Parameters	Value
Bucket Capacity	0.75 m^3
Engine Power	125 kW
Digging Depth	6.0 m
Digging Reach	8.8 m
Operating Weight	15.6 t
Emission Level	EU Stage II

5.2.1 Set Up

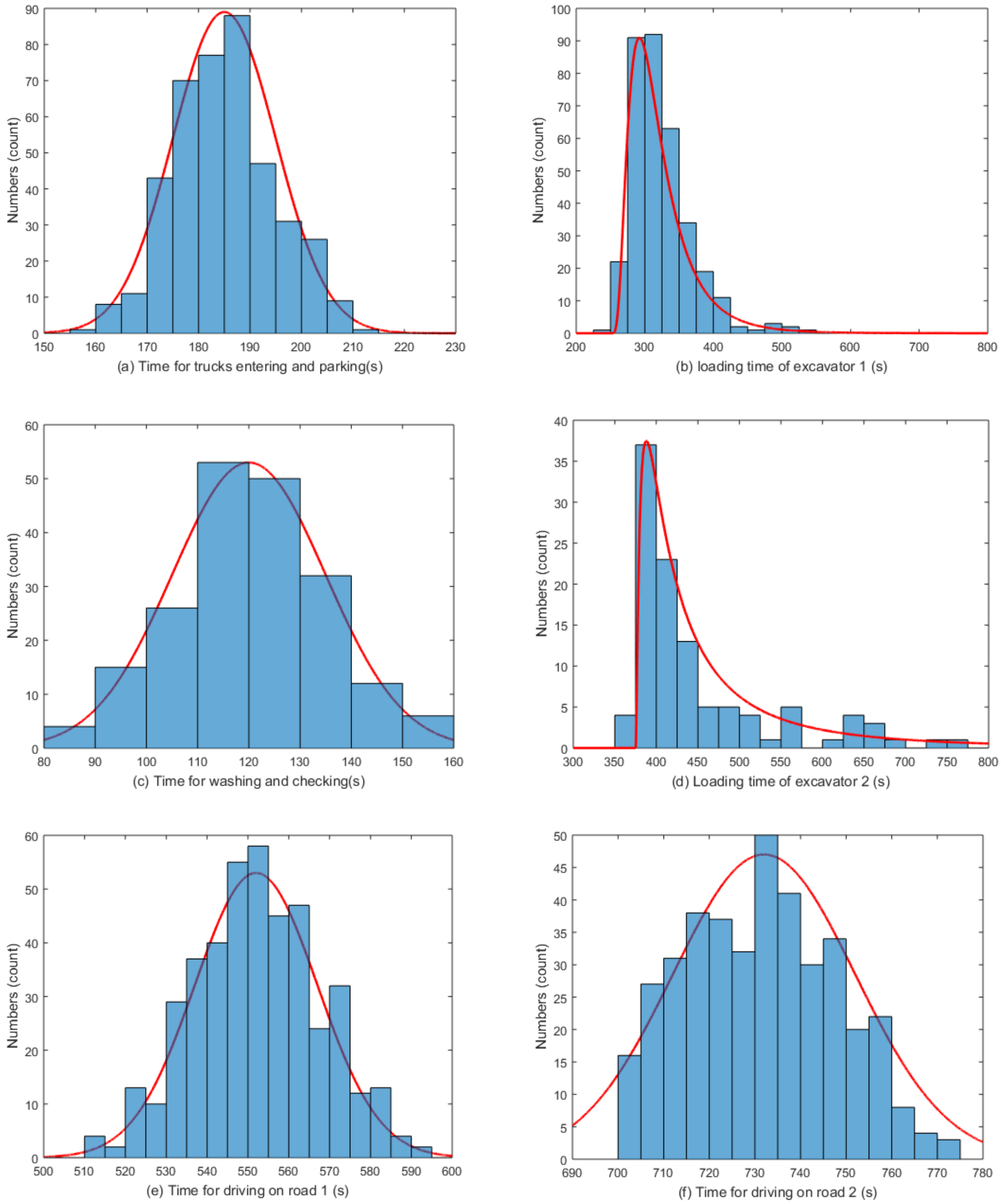

Figure 33 Time distribution of each process

According to the survey logs, the time consumption of each part can be counted. The event numbers are listed in table 23 below. The histograms are constructed by dividing time into series of intervals—and then count how many events fall into each interval. These plots intuitively reveal the features of earthmoving operations. For example, diagram (b) and (d) in figure 33, although their different engine sizes and bucket capacities cause the bias between two kinds of excavators in efficiency, the operation processes of these two excavators are similar: they all concentrate at a certain time interval and very few events can finish sooner than that time.

Particularly, due to the construction regulations, researchers are forbidden to enter the dumping zone. So, the time of dumping is speculated from the GPS data which shows when trucks were stopping in the dumping zone. However the GPS data accuracy only allows us to set the value as a constant number. Moreover, to simplify the simulation, we put some processes as one part, such as: the entering and parking of trucks on construction site, and trucks washing by workers and the spot checking by managers.

Table 23 Statistics for construction processes

Construction Process	Event Counts	Distribution	Parameters (sec)
Entering and Parking	410	Normal	$\mu = 185, \sigma^2 = 10$
Loading by excavator 1	342	Lognormal	$\mu = 5.66, \sigma = 0.14$
Loading by excavator 2	120	Lognormal	$\mu = 6.09, \sigma = 0.71$
Washing and Checking	200	Normal	$\mu = 127, \sigma^2 = 15$
Driving on road 1	427	Normal	$\mu = 552, \sigma^2 = 17.3$
Driving on road 2	427	Normal	$\mu = 723, \sigma^2 = 26$
Dumping	6	Constant Value	2

In order to generate the reasonable time consumption in the DES system, the distribution functions (red curves in figure 33) are introduced to describe the relative likelihood for these random variables. As shown in figure 33, the histograms can be approximated by normal and lognormal distributions as below:

$$\mathcal{N}(x|\mu,\sigma) = \frac{1}{\sigma\sqrt{2\pi}} \exp\left[-\frac{(x-\mu)^2}{2\sigma^2}\right], x > 0 \tag{10}$$

Where μ is the expectation of the normal distribution, and the parameter σ^2 denotes the standard deviation.

$$\mathcal{N}(lnx|\mu,\sigma) = \frac{1}{\sigma\sqrt{2\pi}} \exp\left[-\frac{(lnx-\mu)^2}{2\sigma^2}\right], x > 0 \tag{11}$$

Where the location μ and scale σ parameters can be obtained if the arithmetic mean $\mathrm{E[x]}$ and the arithmetic variance $\mathrm{Var[x]}$ are known; it is simpler if σ is computed first:

$$\mu = \ln(\mathrm{E[x]}) - \frac{1}{2}\sigma^2 \tag{12}$$

$$\sigma = \ln\left(1 + \frac{\mathrm{Var[x]}}{\mathrm{E[x]}^2}\right) \tag{13}$$

Table 23 also provides the information about the approximation. Similar to the case 1, this construction case is divided as three main processes. The dump truck is firstly loaded crushed earth at the loading station by the cooperation of excavator (the washing process is included in this part). Then, it starts driving from the construction site to the dump zone when it completes dumping procedure, and the time cost for waiting in line is also contained by this part. The final process is to dump the crushed earth at the dump station, then return to the central asphalt plant and wait to enter the loading station, after which the next cycle is about to start.

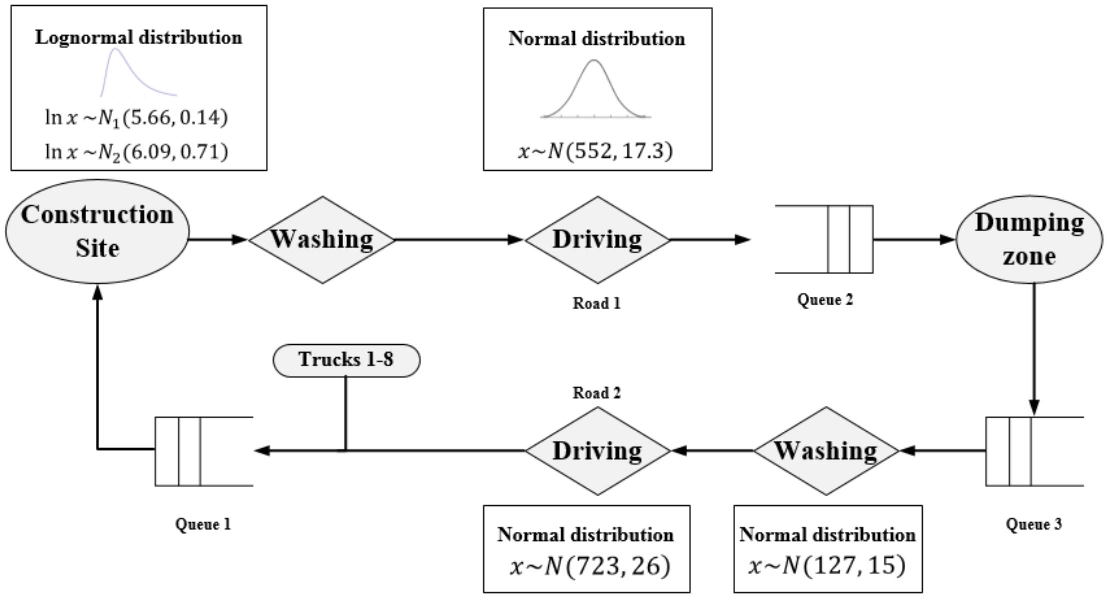

Figure 34 Simulation process for case study (unit: sec)

5.2.2 Simulation Results

Depending on their distribution shape, we assume the loading time obeys the lognormal distribution (see figure 33 (b) and figure 33 (d)). The loading time of these two kinds of excavators is different that concentrate at 4’’39’ and 6’’15 respectively. At the dump station, the dump truck needs some time (almost 2 minutes) for raising and lowering its body, as mentioned before, we assume that the value is constant. Moreover, as demonstrated in figure 33, the time distribution of other parts approximately obeys the normal distribution. In addition, we assume that 8 dump trucks are waiting in the construction site when the simulation starts.

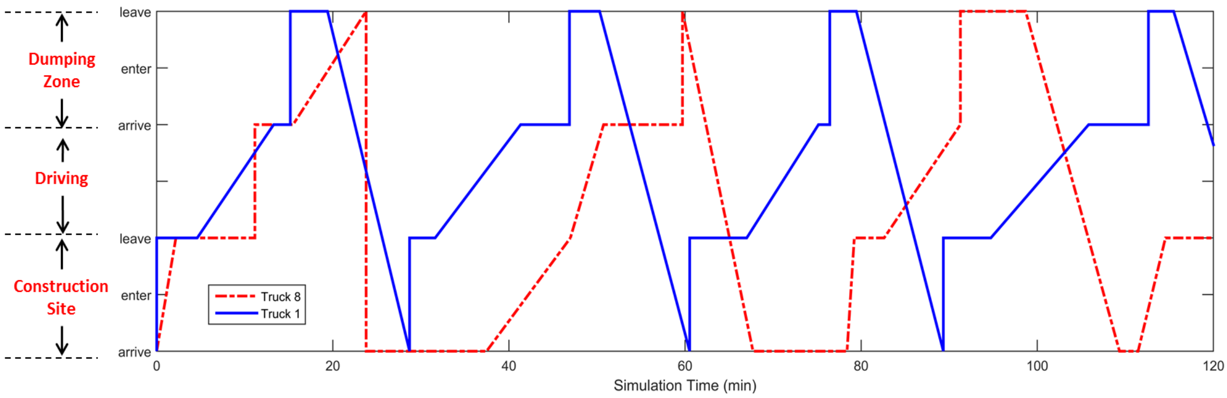

Figure 35 The DES results of truck 1 and truck 8 trajectory

Figure 35 depicts the truck moving trajectory in 120 minutes. Limited by space, we just compare the first (truck 1) and the last one (truck 8), the detailed results are listed in Appendix. At the beginning of the simulation, all eight trucks arrive at the Construction site waiting for loading. Because of the limitation of the number of excavators, only three trucks can start loading at first, and others must wait. After washing and checking, the filled trucks drive to the dumping zone. The unloading process also costs time. Trucks arrive at the construction site and wait for entering until the former truck leaves the three loading stations. The waiting time can be easily observed from the length of horizontal lines. The time difference can be observed because the uncertainty in each process and the form of trucks queue.

6. Conclusions and Future Research

6.1 Conclusions

Within the context in this report, three main tasks have been presented. The first one was the emissions measurement of construction machinery. Test data were logged from engine bench tests and on-board tests. As one of typical non-road machinery, the performance of test loader has been analyzed, and its emission characteristic also been statistically summarized through different test cycles. Similar to the wheel loader, most of construction machinery is repetitive. Typical test modes which represent the original duty-cycles of construction machinery will effectively reflect the relationship between emission and other parameters. The testing method used in this part is available for other equipment, and it also provide an approach to simplify the operation measurement. The second task is the core of this study; the micro-scale emission model has been developed to quantify detailed exhaust NOx emissions from construction equipment (machines and vehicles). Compared to measurement data, the data-driven model result shows good performance in predicting emission.

In addition to model exhaust emissions from heavy construction machine, the last task of the report presents a pre-study for the integration of the emission model with the DES system. The case study of DES system is simulated based on the survey about the construction operations. As the emissions estimation of the whole construction process is a rather new field of research, this part shows the potentiality of DES system for integrating with emission models. The next step DES system with the ability to estimate emissions can optimize the complex construction operations with respect to environmental impacts.

6.2 Future Research

The study in this report is trying to develop a practical method about how to effectively test non-road machinery and how to build dynamic emission based on the on-board test data. However, the study is limited in one single machine type being tested, only a wheel loader without after-treatment system. Both testing and modeling methodology needs further verification with other construction machines. The current Chinese National III non-road emission regulation gives the manufacturer opportunities to develop machine engine for meeting the NOx limit without adding after-treatment system. Therefore, the engine-out emission is the final emission to the air. With the obvious trend of more stringent regulation to be implemented in the future, it is necessary to extend the current emission model with the modeling of after-treatment system. Moreover, sophisticated equipment is also needed for capturing other categories of pollutants in the exhaust gas, and other data-driven emission inventories will be easily added using the same modeling methodology presented in chapter 4.

The last part in this report is the establishment of the DES system, and the integration of the DES system with emission models has not been finished. Although the result of DES simulation shows the flexibility for combining operation process with emission estimation, the current emission model should be more aggregated to accommodate the amount of computation brought by the DES system.

7. Appendix

7.1 Abbreviations

ACD	Activity cycle diagram
AT	After-treatment system
BSFC	Brake specific fuel consumption
CAP	Central asphalt plant
CAN	Controller area network
CH_4	Methane
CI	Compression Ignition (i.e., diesel engines)
CO	Carbon monoxide
CO_2	Carbon dioxide
CRE	common rail engine
DES	Discrete event simulation
DOC	Diesel oxidation catalyst
DPF	Diesel particulate filter
ECU	Engine control unit
EGR	Exhaust gas recirculation
EPA	Environmental protection agency
ESC	European stationary cycle
ETC	European transient cycle
EU	European Union
LPG	Liquefied petroleum gas
g/bhp-hr	Grams per brake horsepower hour
g/kWh	Grams per kilowatt hour
HC	Hydrocarbons
HDD	Heavy-duty diesel
hp	Horsepower
MTV	Material transfer vehicle
NG	Natural gas
NMHC	Non-methane hydrocarbons
NO	Nitrogen oxide
NO_2	Nitrogen dioxide
NOx	Oxides of nitrogen
NRSC	Non-road stationary cycle
NRMM	non-road mobile machinery
PEMS	Portable emissions measurement system
PAHs	polyromantic hydrocarbons
PM	Particulate matter
PN	Particle number limits
ppm	Parts per million
rpm	Revolutions per minute
SCR	Selective catalyst reduction
SI	Spark ignition
SOI	start of injection

7.1 DES Results of Earthmoving Case

Dump truck 1 arrives at the Construction Site at 0.00.
Dump truck 2 arrives at the Construction Site at 0.00.
Dump truck 3 arrives at the Construction Site at 0.00.
Dump truck 4 arrives at the Construction Site at 0.00.
Dump truck 5 arrives at the Construction Site at 0.00.
Dump truck 6 arrives at the Construction Site at 0.00.
Dump truck 7 arrives at the Construction Site at 0.00.
Dump truck 8 arrives at the Construction Site at 0.00.
Dump truck 1 enters the Construction Site at 0.00.
Dump truck 2 enters the Construction Site at 0.00.
Dump truck 3 enters the Construction Site at 0.00.
Dump truck 4 enters the Construction Site at 0.00.
Dump truck 5 enters the Construction Site at 0.00.
Dump truck 6 enters the Construction Site at 0.00.
Dump truck 7 enters the Construction Site at 0.00.
Dump truck 8 enters the Construction Site at 0.00.
Dump truck 1 leaves the Construction Site at 2.18.
Dump truck 6 leaves the Construction Site at 3.54.
Dump truck 7 leaves the Construction Site at 4.19.
Dump truck 5 leaves the Construction Site at 5.57.
Dump truck 2 leaves the Construction Site at 7.03.
Dump truck 3 leaves the Construction Site at 9.21.
Dump truck 4 leaves the Construction Site at 9.83.
Dump truck 1 arrives at the Dumping zone at 11.15.
Dump truck 1 enters the Dumping zone at 11.15.
Dump truck 8 leaves the Construction Site at 11.57.
Dump truck 6 arrives at the Dumping zone at 13.20.
Dump truck 5 arrives at the Dumping zone at 14.55.
Dump truck 2 arrives at the Dumping zone at 15.38.
Dump truck 1 leaves the Dumping zone at 15.49.
Dump truck 6 enters the Dumping zone at 15.49.
Dump truck 7 arrives at the Dumping zone at 15.69.
Dump truck 3 arrives at the Dumping zone at 19.49.
Dump truck 6 leaves the Dumping zone at 19.71.
Dump truck 5 enters the Dumping zone at 19.71.
Dump truck 4 arrives at the Dumping zone at 20.26.
Dump truck 8 arrives at the Dumping zone at 22.24.
Dump truck 5 leaves the Dumping zone at 22.82.
Dump truck 2 enters the Dumping zone at 22.82.
Dump truck 1 returns the Construction Site at 23.78.
Dump truck 1 arrives at the Construction Site at 23.78.
Dump truck 1 enters the Construction Site at 23.78.
Dump truck 2 leaves the Dumping zone at 26.20.
Dump truck 7 enters the Dumping zone at 26.20.
Dump truck 7 leaves the Dumping zone at 30.21.
Dump truck 3 enters the Dumping zone at 30.21.
Dump truck 6 returns the Construction Site at 30.87.
Dump truck 6 arrives at the Construction Site at 30.87.
Dump truck 6 enters the Construction Site at 30.87.
Dump truck 5 returns the Construction Site at 31.42.
Dump truck 5 arrives at the Construction Site at 31.42.
Dump truck 5 enters the Construction Site at 31.42.
Dump truck 6 leaves the Construction Site at 31.91.
Dump truck 3 leaves the Dumping zone at 34.55.
Dump truck 4 enters the Dumping zone at 34.55.

Dump truck 2 returns the Construction Site at 36.62.
Dump truck 2 arrives at the Construction Site at 36.62.
Dump truck 2 enters the Construction Site at 36.62.
Dump truck 1 leaves the Construction Site at 37.46.
Dump truck 4 leaves the Dumping zone at 38.37.
Dump truck 8 enters the Dumping zone at 38.37.
Dump truck 7 returns the Construction Site at 39.67.
Dump truck 7 arrives at the Construction Site at 39.67.
Dump truck 7 enters the Construction Site at 39.67.
Dump truck 8 leaves the Dumping zone at 41.78.
Dump truck 6 arrives at the Dumping zone at 42.86.
Dump truck 6 enters the Dumping zone at 42.86.
Dump truck 5 leaves the Construction Site at 43.34.
Dump truck 3 returns the Construction Site at 45.11.
Dump truck 3 arrives at the Construction Site at 45.11.
Dump truck 3 enters the Construction Site at 45.11.
Dump truck 6 leaves the Dumping zone at 46.14.
Dump truck 1 arrives at the Dumping zone at 46.98.
Dump truck 1 enters the Dumping zone at 46.98.
Dump truck 4 returns the Construction Site at 48.27.
Dump truck 4 arrives at the Construction Site at 48.27.
Dump truck 4 enters the Construction Site at 48.27.
Dump truck 2 leaves the Construction Site at 49.60.
Dump truck 1 leaves the Dumping zone at 50.75.
Dump truck 8 returns the Construction Site at 51.44.
Dump truck 8 arrives at the Construction Site at 51.44.
Dump truck 8 enters the Construction Site at 51.44.
Dump truck 7 leaves the Construction Site at 51.72.
Dump truck 5 arrives at the Dumping zone at 52.22.
Dump truck 5 enters the Dumping zone at 52.22.
Dump truck 3 leaves the Construction Site at 53.56.
Dump truck 5 leaves the Dumping zone at 54.72.
Dump truck 6 returns the Construction Site at 56.23.
Dump truck 6 arrives at the Construction Site at 56.23.
Dump truck 6 enters the Construction Site at 56.23.
Dump truck 4 leaves the Construction Site at 56.63.
Dump truck 2 arrives at the Dumping zone at 57.17.
Dump truck 2 enters the Dumping zone at 57.17.
Dump truck 2 leaves the Dumping zone at 58.98.
Dump truck 1 returns the Construction Site at 59.71.
Dump truck 1 arrives at the Construction Site at 59.71.
Dump truck 1 enters the Construction Site at 59.71.
Dump truck 8 leaves the Construction Site at 60.49.
Dump truck 7 arrives at the Dumping zone at 60.63.
Dump truck 7 enters the Dumping zone at 60.63.
Dump truck 7 leaves the Dumping zone at 63.77.
Dump truck 3 arrives at the Dumping zone at 64.54.
Dump truck 3 enters the Dumping zone at 64.54.
Dump truck 5 returns the Construction Site at 65.02.
Dump truck 5 arrives at the Construction Site at 65.02.
Dump truck 5 enters the Construction Site at 65.02.
Dump truck 6 leaves the Construction Site at 66.10.
Dump truck 4 arrives at the Dumping zone at 67.52.
Dump truck 1 leaves the Construction Site at 67.72.
Dump truck 2 returns the Construction Site at 67.91.
Dump truck 2 arrives at the Construction Site at 67.91.
Dump truck 2 enters the Construction Site at 67.91.

Dump truck 3 leaves the Dumping zone at 68.83.
Dump truck 4 enters the Dumping zone at 68.83.
Dump truck 8 arrives at the Dumping zone at 69.98.
Dump truck 5 leaves the Construction Site at 71.45.
Dump truck 4 leaves the Dumping zone at 72.47.
Dump truck 8 enters the Dumping zone at 72.47.
Dump truck 8 leaves the Dumping zone at 74.41.
Dump truck 7 returns the Construction Site at 74.99.
Dump truck 7 arrives at the Construction Site at 74.99.
Dump truck 7 enters the Construction Site at 74.99.
Dump truck 2 leaves the Construction Site at 75.00.
Dump truck 6 arrives at the Dumping zone at 77.38.
Dump truck 6 enters the Dumping zone at 77.38.
Dump truck 1 arrives at the Dumping zone at 78.40.
Dump truck 6 leaves the Dumping zone at 79.22.
Dump truck 1 enters the Dumping zone at 79.22.
Dump truck 3 returns the Construction Site at 79.91.
Dump truck 3 arrives at the Construction Site at 79.91.
Dump truck 3 enters the Construction Site at 79.91.
Dump truck 5 arrives at the Dumping zone at 80.71.
Dump truck 4 returns the Construction Site at 81.66.
Dump truck 4 arrives at the Construction Site at 81.66.
Dump truck 4 enters the Construction Site at 81.66.
Dump truck 7 leaves the Construction Site at 82.58.
Dump truck 1 leaves the Dumping zone at 82.61.
Dump truck 5 enters the Dumping zone at 82.61.
Dump truck 5 leaves the Dumping zone at 85.63.
Dump truck 8 returns the Construction Site at 85.82.
Dump truck 8 arrives at the Construction Site at 85.82.
Dump truck 8 enters the Construction Site at 85.82.
Dump truck 2 arrives at the Dumping zone at 86.49.
Dump truck 2 enters the Dumping zone at 86.49.
Dump truck 6 returns the Construction Site at 88.00.
Dump truck 6 arrives at the Construction Site at 88.00.
Dump truck 6 enters the Construction Site at 88.00.
Dump truck 3 leaves the Construction Site at 89.75.
Dump truck 1 returns the Construction Site at 91.27.
Dump truck 1 arrives at the Construction Site at 91.27.
Dump truck 1 enters the Construction Site at 91.27.
Dump truck 2 leaves the Dumping zone at 91.61.
Dump truck 7 arrives at the Dumping zone at 91.96.
Dump truck 7 enters the Dumping zone at 91.96.
Dump truck 8 leaves the Construction Site at 93.96.
Dump truck 5 returns the Construction Site at 94.94.
Dump truck 5 arrives at the Construction Site at 94.94.
Dump truck 5 enters the Construction Site at 94.94.
Dump truck 7 leaves the Dumping zone at 95.42.
Dump truck 4 leaves the Construction Site at 95.64.
Dump truck 6 leaves the Construction Site at 98.16.
Dump truck 3 arrives at the Dumping zone at 98.62.
Dump truck 3 enters the Dumping zone at 98.62.
Dump truck 1 leaves the Construction Site at 98.68.
Dump truck 3 leaves the Dumping zone at 101.03.
Dump truck 2 returns the Construction Site at 101.53.
Dump truck 2 arrives at the Construction Site at 101.53.
Dump truck 2 enters the Construction Site at 101.53.
Dump truck 2 leaves the Construction Site at 101.93.

Dump truck 8 arrives at the Dumping zone at 103.52.
Dump truck 8 enters the Dumping zone at 103.52.
Dump truck 7 returns the Construction Site at 104.76.
Dump truck 7 arrives at the Construction Site at 104.76.
Dump truck 7 enters the Construction Site at 104.76.
Dump truck 4 arrives at the Dumping zone at 105.26.
Dump truck 8 leaves the Dumping zone at 105.92.
Dump truck 4 enters the Dumping zone at 105.92.
Dump truck 6 arrives at the Dumping zone at 106.88.
Dump truck 5 leaves the Construction Site at 108.04.
Dump truck 4 leaves the Dumping zone at 108.46.
Dump truck 6 enters the Dumping zone at 108.46.
Dump truck 1 arrives at the Dumping zone at 109.34.
Dump truck 2 arrives at the Dumping zone at 111.26.
Dump truck 3 returns the Construction Site at 111.40.
Dump truck 3 arrives at the Construction Site at 111.40.
Dump truck 3 enters the Construction Site at 111.40.
Dump truck 6 leaves the Dumping zone at 111.45.
Dump truck 1 enters the Dumping zone at 111.45.
Dump truck 7 leaves the Construction Site at 112.29.
Dump truck 1 leaves the Dumping zone at 114.56.
Dump truck 2 enters the Dumping zone at 114.56.
Dump truck 8 returns the Construction Site at 116.31.
Dump truck 8 arrives at the Construction Site at 116.31.
Dump truck 8 enters the Construction Site at 116.31.
Dump truck 2 leaves the Dumping zone at 118.07.
Dump truck 4 returns the Construction Site at 119.15.
Dump truck 4 arrives at the Construction Site at 119.15.
Dump truck 4 enters the Construction Site at 119.15.
Dump truck 3 leaves the Construction Site at 119.48.
Dump truck 5 arrives at the Dumping zone at 119.82.
Dump truck 5 enters the Dumping zone at 119.82.

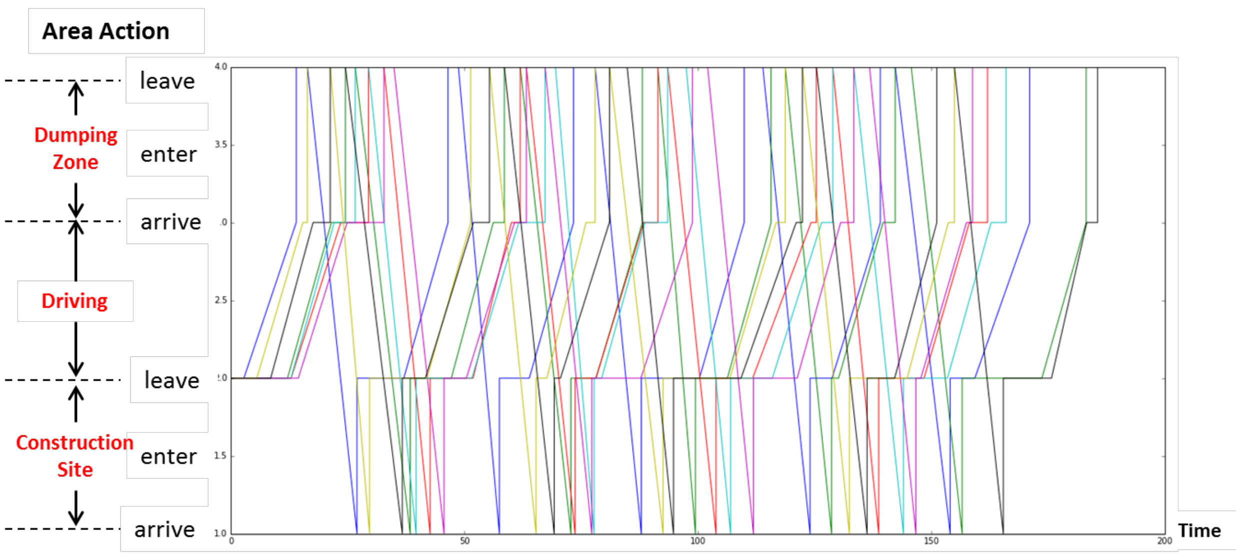

Figure 35 The DES results of trucks trajectory

8. Reference

1. Hughes, Phil, and Ed Ferrett. Introduction to health and safety in construction. Routledge, 2012: pp. 186-189.
2. Midwest Research Institute. Estimating particular matter emissions from construction operations. EPA 68D7-0068. United States Environmental Protection Agency. 1999.
3. Johnson, Timothy. Vehicular emissions in review. SAE International Journal of Engines (7.2014-01-1491) 2014: 1207-1227.
4. Wang, Linlin, David T. Allen, and Elena C. McDonald-Buller. Air quality modeling of interpollutant trading for ozone precursors in an urban area. Journal of the Air & Waste Management Association 55, no. 10 (2005): 1543-1557.
5. Directive 2008/1/EC of the European Parliament and of the Council of 15 January 2008 concerning integrated pollution prevention and control (codified version) Official Journal of the European Union (2008) L 24/8
6. CHEN, Hu, Wen-miao CHEN, Jian-xin WANG, and Shi-jin SUAI. Study on PM Emission Characteristics of Diesel Engine Fueled with Ethanol-Diesel Blend [J]." Transactions of CSICE 4 (2005): 002.
7. Health Aspects of Air Pollution with Particulate Matter, Ozone and Nitrogen Dioxide. World Health Organization. 13–15 January 2003. p. 48. Retrieved 2011-11-19.
8. U.S. EPA. National Clean Diesel Campaign. National Funding Assistance Program, U.S. 13 Environmental Protection Agency, available at www.epa.gov/cleandiesel/prgnational. 2012.
9. EU Regulation (EC) No 715/2007 of the European Parliament and of the Council of 20 June 2007 on type approval of motor vehicles with respect to emissions from light passenger and commercial vehicles (Euro 5 and Euro 6) and on access to vehicle repair and maintenance information. Official Journal of the European Union. Retrieved 2011-02-02.
10. EU Amending Directive 97/68/EC of the European Parliament and of the Council on the approximation of the laws of the Member States relating to measures against the emission of gaseous and particulate pollutants from internal combustion engines to be installed in non-road mobile machinery, Official Journal of the European Union. Retrieved 2012-12-21.
11. DieselNet (2012). Emission Standards: Summary of Worldwide Emission Standards. Available at: www.dieselnet.com/standards/. Accessed 29 July 2013.
12. Fiori Group (2014). Detailed implementation dates and emission levels in accordance with the EU and EPA regulations. Available at http://www.fiorigroup.com/products/engine-emissions/eu-and-epa/. 2015.
13. EU Directive 2000/25/EC of the European Parliament and of the Council of 22 May 2000 on action to be taken against the emission of gaseous and particulate pollutants by engines intended to power agricultural or forestry tractors and amending Council Directive 74/150/EEC European Union Official Journal, L173 (2000) (2000), pp. 1–34

14. EU Directive 2004/26/EC of the European Parliament and of the Council of 21 April 2004 on the approximation of the laws of the Member States relating to measures against the emission of gaseous and particulate pollutants from internal combustion engines to be installed in non-road mobile machinery. European Union Official Journal, L146 (2004). 2004, pp. 1–107
15. EU Commission Directive 2005/13/EC of 21 February 2005 amending Directive 2000/25/EC of the European Parliament and of the Council concerning the emission of gaseous and particulate pollutants by engines intended to power agricultural or forestry tractors, and amending Annex I to Directive 2003/37/EC of the European Parliament and of the Council concerning the type-approval of agricultural or forestry tractors. European Union Official Journal, L55 (2005). 2005, pp. 35–54
16. CHINA EPB. Limits and measurement methods for exhaust pollutants from diesel engines of non-road mobile machinery (CHINA III, IV) (GB 20891-2014). 2014
17. EPA U.S. User's guide to MOBILE6.1 and MOBILE6.2. Mobile source emission factor model. EPA420-R-03-010. United States Environmental Protection Agency. 2003.
18. Ekström M, Sjödin Å, Andreasson K. Evaluation of the COPERT III emission model with on-road optical remote sensing measurements. Atmospheric Environment, 2004, 38(38): 6631-6641.
19. University of California at Riverside. IVE Model User Manual Version 2.0 http://www.issrc.org/ive/downloads/manuals/UsersManual.pdf
20. Keller, M., N. Kljun, ARTEMIS Road Emission Model User Guide. EU Commission, 2007
21. Rakha, H., K. Ahn, & A. Trani, Development of VT-Micro model for estimating hot stabilized light duty vehicle and truck emission. Transportation Research Part D, 9, 49–74, 2004.
22. Barth M, F. An, T. Younglove, Comprehensive modal emission model (CMEM), version 2.0 user's guide. University of California, Riverside, 2000.
23. Arrègle J, J. Javier López, C. Guardiola, C. Monin, On board NOx prediction in diesel engines: a physical approach. Automotive Model Predictive Control. Chapter 2, Springer London, 2010: 25-36.
24. Boriboonsomsin, Kanok, and Matthew Barth. "Evaluating air quality benefits of freeway high-occupancy vehicle lanes in Southern California." Transportation Research Record: Journal of the Transportation Research Board (2015).
25. Lewis, P., H. Frey, and W. Rasdorf. Development and use of emissions inventories for construction vehicles. Transportation Research Record: Journal of the Transportation Research Board, No. 2123, Transportation Research Board of the National Academies, Washington, D.C., 2009, pp. 46-53.
26. Abolhasani, Saeed, Real-world in-use activity, fuel use, and emissions for nonroad construction vehicles: a case study for excavators. Journal of the Air & Waste Management Association 58.8 (2008): 1033-1046.
27. EPA U.S. MOVES 2014 User's guide. EPA-420-B-14-055. United States Environmental Protection Agency. 2014.

28. P Lewis, A Hajji, Case Study of an Energy and Environmental Inventory for a Municipal Heavy Duty Diesel Equipment Fleet. Transportation Research Board 93rd Annual Meeting. 2014 (paper no.14-4561).
29. Quérel C, O. Grondin, C. Letellier, A Semi-Physical NOx Model for Diesel Engine Control. SAE Technical Paper, 2013.
30. Singh N, P. Nagabushan-Venkatesh, E. Nigro, Development of the NOx Emission Model for the Heavy Duty Diesel Engine Application Using Combustion Characteristic Parameters. SAE Technical Paper, 2013.
31. Moridis G J. Toward production from gas hydrates: current status, assessment of resources, and simulation-based evaluation of technology and potential. Lawrence Berkeley National Laboratory, 2008.
32. Song, Lingguang, Fernando Ramos, and Katie Arnold. A framework for real-time simulation of heavy construction operations. In *Proceedings of the 40th Conference on Winter Simulation*, pp. 2387-2395. Winter Simulation Conference, 2008.
33. Lau, Sze-Chun, Ming Lu, and Chi-Sun Poon. "Formalized Approach to Discretize a Continuous Plant in Construction Simulations." Journal of Construction Engineering and Management 140.8 (2014): 04014032. 2014.
34. Ioannou P G, Martinez J C. Simulation of complex construction processes. Proceedings of the 28th conference on Winter simulation. IEEE Computer Society, 1996: 1321-1328.
35. Zhao X, C. Schindler, Evaluation of whole-body vibration exposure experienced by operators of a compact wheel loader according to ISO 2631-1: 1997 and ISO 2631-5: 2004. International Journal of Industrial Ergonomics, 2014, 44(6): 840-850.
36. Ma, X., W. Lei, I. Andréasson, H. Chen, An evaluation of microscopic emission models for traffic pollution simulation using on-board measurement. Environmental Modeling & Assessment, 2012, 17(4): 375-387.
37. Mansharamani R. An overview of discrete event simulation methodologies and implementation. Sadhana. 1997, 22(5):611-27.
38. Ritchie Bros. VOLVO a25d articulated dump truck. Available at http://www.ritchiespecs.com/specification?category=Articulated%20Dump%20Truck&make=VOLVO&model=a25d&modelid=97712
39. Volvo Construction Equipment. Volvo L60G, L70G, L90G Wheel Loaders: The capacity and flexibility to load on more work. Available at http://www.volvoce.com/constructionequipment/na/en-us/products/wheelloaders/wheelloaders/L60G_L70G_L90G/Pages/featuresandbenefits.aspx
40. Yin, Zhimin. Advanced Quantitative Techniques to Enhance Heavy and Civil Construction Information Modeling. PhD Diss. University of Alberta, 2011.